

Evaluation of circular orbits and innermost stable circular orbits of neutral and charged particles around black holes

Eahsaan Nazir Najar* and Raja Nisar Ali†
*Physics Department, School of Physical and Chemical Sciences,
Central University of Kashmir, J&K-191131, India*

Yasmeena Mushtaq‡
Department of Physics, National Institute of Technology, Srinagar, J&K-190006, India

Imtiyaz Ahmad Bhat§
Department of Physics, Islamic University of Science and Technology, Awantipora, J&K-192122, India
(Dated: March 13, 2026)

In this paper we study the effective gravitational potential of Schwarzschild, Kerr, Reissner-Nordström and Kerr-Newman black holes with the relativistic corrections to evaluate the circular orbits and the Innermost Stable Circular Orbits (ISCOs) —a purely relativistic phenomenon— of neutral and charged particles in the vicinity of these spacetimes. We study the circular orbits and ISCOs of black holes mathematically and graphically. Moreover, the astrophysical properties of ISCO are also dealt with. We find that the particle entering the ISCO loses a certain amount of energy, in different spacetimes, by gravitational radiative processes, before finally spiraling into ISCO. The electromagnetic effects of different spacetimes show how the charges sharpen the radius of the circular orbits, and the increasing product of particle and black hole charge increases the radius of the ISCO. Most importantly, the effective potential of the most general spacetime, as predicted by the no-hair conjecture, has been derived.

I. INTRODUCTION

Among all the physically plausible causal structures, black holes are the most fascinating and relativistically interesting ones. We study black holes through their interactions with surrounding matter or via their spacetime deformations outside the event horizons: the causal boundary between events that can communicate with distant observers and events that cannot [1–3]. Black holes are interesting for being one of the possible end-points of stellar evolution, they are the power feeders of quasars and active galactic nuclei and are, nevertheless, the most mysterious macroscopic objects in the universe. It is possible to study them in a way, with mathematical rigor, that is almost impossible for any other stellar system; our interest, however, is in relativistic kinematic effects.

In this article we explore the circular orbits and ISCOs of neutral and charged particles in the gravitational field of Schwarzschild, Kerr, Reissner-Nordström, and Kerr-Newman black holes. ISCOs represent the region between test particles orbiting the black hole and particles falling into the black hole; therefore, they are an important tool for studying the physics of accretion disk [4, 5]. Initially we analyze the geometry of the Schwarzschild spacetime II [6] followed by the circular orbits and ISCOs of neutral particles in the Schwarzschild black hole II A;

where the black hole has been assumed to be charge neutral [7]; because black holes are widely considered charge neutral as shortly after the accretion of ambient matter neutralizes all excess charges. But we have strong reasons to believe that weakly charged black holes exist [8–11] and the electromagnetic coupling of the black hole charge and test particle charge is dealt with in section II B.

The Schwarzschild black holes are non rotating, so we next study the Kerr black holes; section III. The circular orbits and ISCOs of neutral particles in the vicinity of Kerr spacetime are evaluated in section III A. The problem of interaction of black hole charge and test particle charge in the Kerr spacetime is the subject matter of section III B; here we have studied the ISCOs of charged particles immersed in an axisymmetric magnetic field [7, 12].

Next we study Reissner-Nordström, another important class of black holes, section IV; followed by the study of circular orbits and ISCOs of neutral particles in the vicinity of Reissner-Nordström spacetime, section IV A and ISCOs of charged particles in Reissner-Nordström black hole spacetime IV B. We calculated the effective potential of the Reissner-Nordström spacetime.

Finally, we investigated the problem of Kerr-Newman black hole [5, 13, 14]: geometry, circular orbits, and ISCOs of neutral particles, respectively, in sections V and V A. We have derived the most effective gravitational potential of a black hole as stated by the no-hair conjecture —a stationary black hole parameterization is done solely by three parameters: mass, charge, and angular Momentum— because in Kerr-Newmann spacetimes, contrary to Schwarzschild, Kerr, and Reissner-Nordstrom spacetimes, all three parameters, stated above, are

* eahsaan.phy@gmail.com

† rjnisar@cukashmir.ac.in

‡ yasmeena746@gmail.com

§ bhat.imtiyaz@iust.ac.in

nonzero. Thus, the Kerr-Newmann black hole according to the no-hair theorem is the most general stationary solution to Einstein's field equations.

We use the sign conventions adopted by [1] and the speed of light(c), the universal gravitational constant(G) and the Coulomb's constant(k) are unity.

II. SCHWARZSCHILD BLACK HOLE

The general theory of relativity with regard to the spacetime structure of the cosmos has made a number of stunningly successful predictions. Our solar system is the most feasible and easily accessible lab to validate these predictions. Thus, determining the solutions of Einstein's equations in the external gravitational field of a static, asymptotically flat, and spherically symmetric body is of immense importance. The first solution was published by Karl Schwarzschild [15] (for a delightful history, see [16]), just after Einstein published his vacuum field equations. The Schwarzschild solution unquestionably remains one of the most important known exact solutions of Einstein's equations.

The Schwarzschild solution as derived by the tetrad method gives the Schwarzschild metric in its final form as,

$$ds^2 = -\left(1 - \frac{2M}{r}\right)dt^2 + \left(1 - \frac{2M}{r}\right)^{-1} dr^2 + r^2 d\Omega^2, \quad (1)$$

where $d\Omega^2 = (d\theta^2 + \sin^2\theta d\phi^2)$ [17]. The metric's mathematical description has two singularities, or points where it seems to blow up or become undefined [18]. First, the curvature singularity ($r = 0$): at the very center of the black hole, where the curvature of spacetime becomes infinite. This is a true, physical singularity where the theory of general relativity breaks down. Second, the coordinate singularity ($r_S = 2M$): this is the Schwarzschild radius where the metric appears to have defects. But this is the fault of the coordinate system, and the spacetime is actually smooth at this boundary. Other coordinate systems (like Kruskal-Szekeres coordinates) show this clearly.

Ordinary bodies for which the Schwarzschild radius r_S is well within the radius of the body, such as the Sun or planets, the vacuum Schwarzschild solution is no longer valid. Evidently, the physical and coordinate singularities, as defined above, are relevant to spacetimes with event horizons or bodies that have undergone gravitational collapse.

A. Circular orbits of gravitating neutral particles in Schwarzschild black hole

In this section, we will analyze the behavior of test charged particles in the exterior region ($r > 2M$) of the Schwarzschild solution by solving for the timelike and null geodesics of the Schwarzschild geometry.

Let a test particle of mass m be moving with four-velocity u^μ in the Schwarzschild background. Since, the Schwarzschild metric exhibits two Killing fields —temporal and azimuthal —as the metric is temporally and azimuthally symmetric [7]. They read, respectively, as

$$\psi^\mu = \left(\frac{\partial}{\partial t}\right)^\mu \quad \text{and} \quad \chi^\mu = \left(\frac{\partial}{\partial \phi}\right)^\mu. \quad (2)$$

Corresponding, respectively, to these two Killing fields, there are the following two constants of the particle's motion associated with them

$$\mathcal{E} = -g_{\mu\nu}\psi^\mu u^\nu = -\frac{p_\mu\psi^\mu}{m} = \left(1 - \frac{2M}{r}\right)\dot{t}, \quad (3)$$

and

$$\mathcal{L} = g_{\mu\nu}\chi^\mu u^\nu = \frac{p_\mu\chi^\mu}{m} = (r^2 \sin^2\theta)\dot{\phi}, \quad (4)$$

where $p^\mu = mu^\mu$ is the particle's four-momentum and the two constants of motion \mathcal{E} and \mathcal{L} are the specific energy and the specific azimuthal angular momentum, respectively. Using them along with the normalization $g_{\mu\nu}u^\mu u^\nu = -1$, we reduce the radial equation of motion in the equatorial sub-manifold (where $\theta = \frac{\pi}{2}$ and $\dot{\theta} = 0$) to quadrature:

$$\dot{r}^2 = \mathcal{E}^2 - V(r).$$

Everywhere in this paper, the over-dot denotes differentiation with respect to the particle's proper time. The explicit form reads

$$\frac{1}{2}\mathcal{E}^2 = \frac{1}{2}\dot{r}^2 + \frac{1}{2}\left(1 - \frac{2M}{r}\right)\left(\frac{\mathcal{L}^2}{r^2} + 1\right). \quad (5)$$

Hence, the effective potential $V(r)$ is

$$V(r) = \frac{1}{2} - \frac{M}{r} + \frac{\mathcal{L}^2}{2r^2} - \frac{M\mathcal{L}^2}{r^3}. \quad (6)$$

For the potential to be extremum, the first derivative of the effective potential V must vanish, which leads to

$$Mr^2 - \mathcal{L}^2 r + 3M\mathcal{L}^2 = 0. \quad (7)$$

Clearly, the roots of (7) are

$$r_\pm = \frac{\mathcal{L}^2 \pm \sqrt{\mathcal{L}^4 - 12M^2\mathcal{L}^2}}{2M}. \quad (8)$$

Evidently, if $\mathcal{L}^2 < 12M^2$, there are no physically plausible maxima or minima of $V(r)$. But, if $\mathcal{L}^2 > 12M^2$, we have verified that r_+ is a minima of V , while r_- is a maxima, as illustrated in the figure 1.

Now, for the circular motion, we have $\dot{r} = 0$, hence

$$\mathcal{E}^2 = V = \left(1 - \frac{2M}{r}\right)\left(\frac{\mathcal{L}^2}{r^2} + 1\right) \quad (9)$$

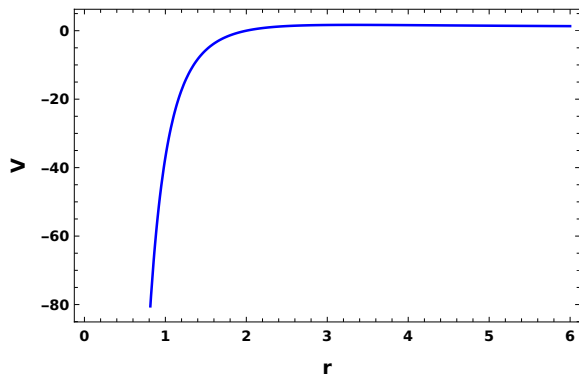


FIG. 1. Variation of potential energy with radius in a Schwarzschild spacetime.

and $V'(r) = 0$ implies

$$Mr^2 - \mathcal{L}^2 r + 3M\mathcal{L}^2 = 0 \quad (10)$$

and the solution of this quadratic equation gives

$$\mathcal{E} = \frac{r - 2M}{\sqrt{r(r - 3M)}} \quad \text{and} \quad \mathcal{L} = \frac{r\sqrt{M}}{\sqrt{r - 3M}} \quad (11)$$

A relativistically and astrophysically interesting phenomenon exhibited by particles in the gravitational field of black holes is the existence of Innermost Stable Circular Orbit (ISCO), which represents a limiting boundary of a particle revolving around a black hole from the test particles falling into the black hole. The condition for ISCO is $V''(r) = 0$, which implies

$$V''(r) = \frac{-2M}{r^3} + \frac{3\mathcal{L}^2}{r^4} - \frac{12M\mathcal{L}^2}{r^5} = 0. \quad (12)$$

Using \mathcal{L}^2 obtained in (11) in equation (12) implies $r = 6M$. We call this r as r_{ISCO} . The general results of ISCO of the Schwarzschild black hole obtained by substituting r_{ISCO} instead of r into equation (11) give the following result.

$$r_{ISCO} = 6M. \quad (13)$$

So, the specific energy of a particle entering the ISCO of a Schwarzschild black hole is

$$\mathcal{E}_{ISCO} = \frac{6M - 2M}{\sqrt{6M(6M - 3M)}} = \frac{4}{\sqrt{18}} \approx 0.942. \quad (14)$$

The energy lost by a particle entering the ISCO is equal to $1 - \mathcal{E}_{ISCO} \approx 0.057$. The angular momentum of the particle entering the ISCO of a Schwarzschild black hole is

$$\mathcal{L}_{ISCO} = \frac{6M\sqrt{M}}{\sqrt{6M - 3M}} = 2\sqrt{3}M. \quad (15)$$

An important and very suggestive point that can be conceived from the equation (14) is that a particle will release 5.7% of its mass energy at rest before finally spiraling into r_{ISCO} . This also suggests that, indeed, by gravitational radiative processes, in the astrophysically plausible phenomenon, large amounts of energy can be radiated.

B. ISCO of charged particles in Schwarzschild black hole

After discussing the relativistic properties of neutral particles in the Schwarzschild black hole, we are in a position to discuss the electrodynamic properties of charged particles. Let us now review Wald's solution of Maxwell equations in a curved spacetime for weak electromagnetic fields [12]. In a Ricci flat spacetime, a Killing vector χ_μ obeys the equation

$$\chi_{\mu;\alpha}{}^{;\alpha} = 0. \quad (16)$$

Consider an electromagnetic potential constructed by the temporal and azimuthal Killing vectors of the Schwarzschild geometry, like

$$A^\mu = -\frac{Q}{2M}\psi_{(t)}^\mu + \frac{B}{2}\psi_{(\phi)}^\mu, \quad (17)$$

where Q is the black hole charge and B is the axisymmetric magnetic field of the black hole. The dynamics of a charged particle of mass m and charge e in an electromagnetic field described by a Minkowskian spacetime is, setting velocity of light equal to 1, governed by the equation

$$m \frac{du^\alpha}{ds} = eF^{\alpha\beta}u_\beta. \quad (18)$$

In an electromagnetic field described by a curved spacetime, the massive charges follow the dynamical equation

$$mu^\beta u^\alpha{}_{;\beta} = eF^{\alpha\gamma}u_\gamma. \quad (19)$$

The electromagnetic field tensor is the same in both Minkowskian and curved spacetimes, and the form is

$$F^{\mu\nu} = \partial^\mu A^\nu - \partial^\nu A^\mu = A^{\nu;\mu} - A^{\mu;\nu}. \quad (20)$$

Due to the azimuthal and temporal symmetries, by Noether's theorem, the specific energy and angular momentum are therefore, respectively, the constants of motion

$$\mathcal{E} = -\frac{p_\mu \psi_{(t)}^\mu}{m} = \frac{q}{r} + \left(1 - \frac{2M}{r}\right) \dot{t} \quad (21)$$

and

$$\mathcal{L} = \frac{p_\mu \psi_{(\phi)}^\mu}{m} = r^2 (b + \dot{\phi}) \sin^2 \theta. \quad (22)$$

Where we have set $q = eQ/m$ and $b = eB/2m$. In an equatorial sub-manifold, the radial equation of motion takes the form

$$\dot{r}^2 = (\mathcal{E} - V_+)(\mathcal{E} - V_-), \quad (23)$$

and the potential reads

$$V_\pm(r) = \frac{q}{r} \pm \sqrt{\left\{1 + \left(\frac{\mathcal{L}}{r} - br\right)^2\right\} \left(1 - \frac{2M}{r}\right)}. \quad (24)$$

The V_+ is potential in the chronologically forward direction, while as V_- is in the chronologically backward direction.

In this paper we have confined our work to the weak field approximation. These approximations break down when the fields produce curvatures comparable to the curvature produced by the black holes' mass near the event horizon. This happens when

$$B^2 \sim M^{-2} \quad \text{or} \quad Q^2 \sim M^2, \quad (25)$$

see [7]. Throughout this paper, these approximations have been carefully taken into account.

Now we can write the expressions of specific energy and angular momentum of charges in circular orbits and ISCOs of Schwarzschild black holes. If we set the magnetic field $b = 0$ in equation (24), we have

$$V_+(r) = \frac{q}{r} + \sqrt{\left(1 + \frac{\mathcal{L}^2}{r^2}\right)\left(1 - \frac{2M}{r}\right)}, \quad (26)$$

which gives the effective, chronologically forward, potential of a particle in a non magnetic black hole. The necessary conditions for circular orbits are $V(r) = \mathcal{E}$ and $V'(r) = 0$. Let us denote the radius of the circular orbit by r_0 . This set of simultaneous equations result in

$$\mathcal{E}_0 = \frac{q}{r_0} + \sqrt{\left(1 + \frac{\mathcal{L}_0^2}{r_0^2}\right)\left(1 - \frac{2M}{r_0}\right)} \quad (27)$$

as the specific energy, and

$$\mathcal{L}_0^2 = \frac{2Mr_0^2}{r_0 - 3M} + \left[\frac{qr_0(r_0 - 2M)}{(r_0 - 3M)^2} \left\{ q - \sqrt{4r_0(r_0 - 3M) + q^2} \right\} \right] \quad (28)$$

as the specific angular momentum.

In an innermost stable circular orbit, the necessary condition is that the second derivative of the potential must vanish, i.e.,

$$\begin{aligned} & \left[r_{ISCO}(\mathcal{L}_0^2 + r_{ISCO}^2)(r_{ISCO} - 2M) \right]^{\frac{1}{2}} \left\{ \mathcal{L}_0^2 - 2Mr_{ISCO} \right\} \\ & + q \left[\mathcal{L}_0^2(r_{ISCO} - M) + r_{ISCO}^2(2r_{ISCO} - 3M) \right] = 0. \quad (29) \end{aligned}$$

By the evaluation of this equation we have explicitly found the variation of r_{ISCO} due to the curvature produced by charges, i.e.,

$$r_{ISCO} = 6M + \frac{q^2}{2M} + O(q^3), \quad (30)$$

see [7]. We can conclude that whenever $|q| > 0$ we have $r_{ISCO} > 6M$. The behavior of the radius, the specific energy, and the specific angular momentum w.r.t. the charge q/M is shown in Fig.2.

Now the second part of our problem is to switch on the magnetic field i.e., to set $b \neq 0$ and simultaneously switch

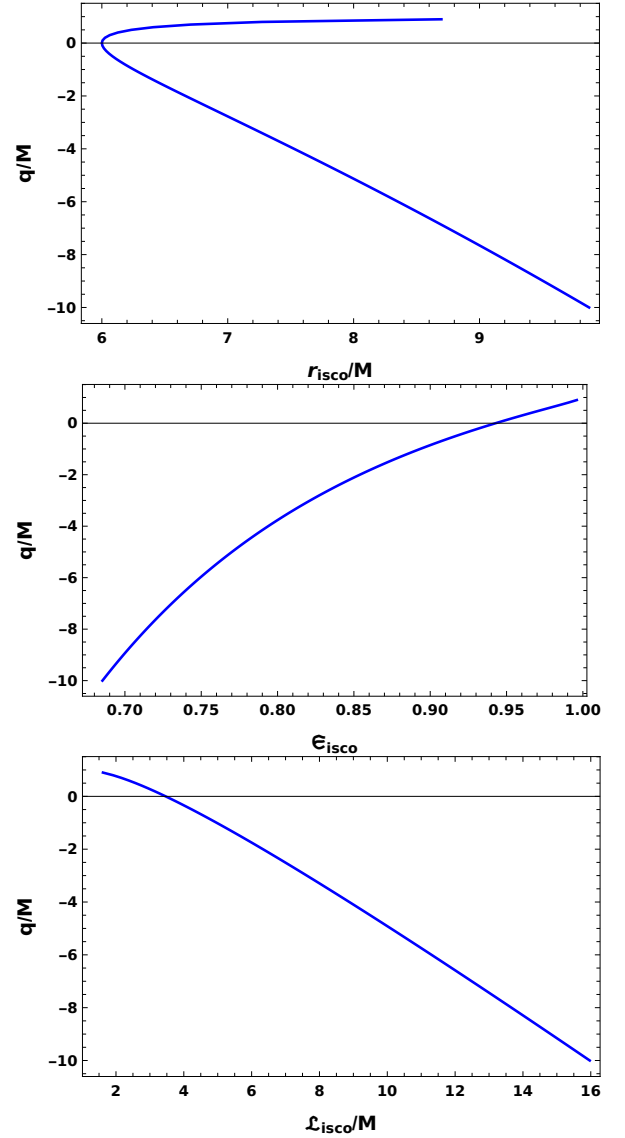


FIG. 2. Variation of : r_{ISCO}/M w.r.t. q/M (Top), \mathcal{E}_{ISCO} w.r.t. q/M (Center) and \mathcal{L}_{ISCO}/M w.r.t. q/M (Bottom).

off the electric field i.e., to set $q = 0$. The potential (24) will take the form

$$V_+(r) = \sqrt{\left\{1 + \left(\frac{\mathcal{L}}{r} - br\right)^2\right\}\left(1 - \frac{2M}{r}\right)}. \quad (31)$$

In the same manner as before, invoking the same conditions, i.e., $V(r) = \mathcal{E}$ and $V'(r) = 0$, we can find explicit expressions for specific energy \mathcal{E} and specific angular momentum \mathcal{L} . The expression for energy reads

$$\mathcal{E}_0 = \sqrt{\left\{1 + \left(\frac{\mathcal{L}_0}{r_0} - br_0\right)^2\right\}\left(1 - \frac{2M}{r_0}\right)} \quad (32)$$

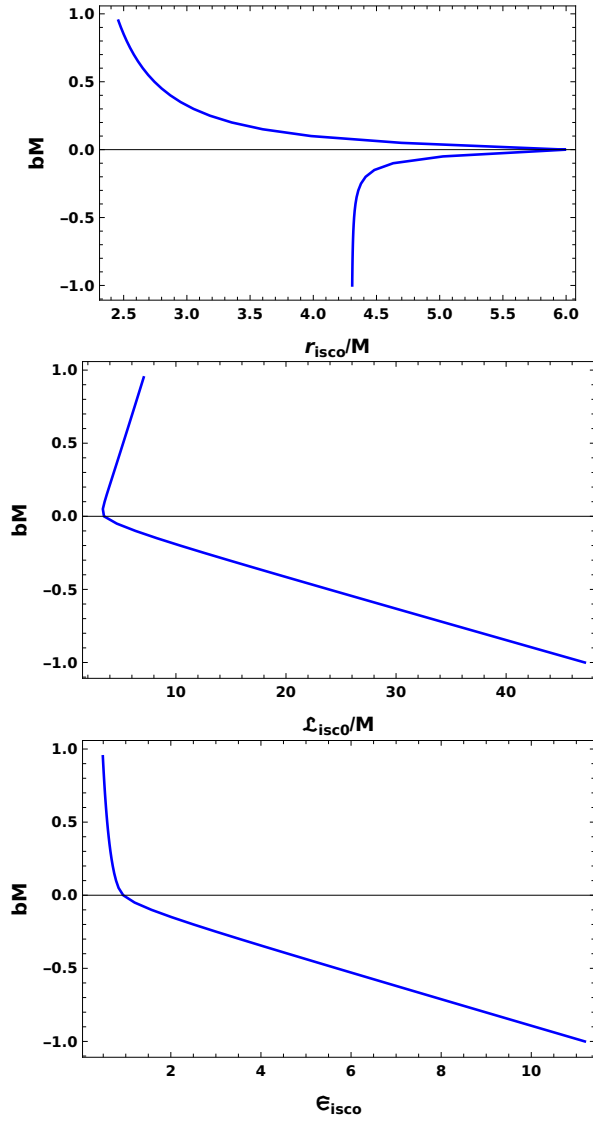


FIG. 3. Variation of : radius r_{ISCO}/M w.r.t. magnetic parameter bM (Top), specific energy \mathcal{E}_0 w.r.t. bM (Center) and specific angular momentum \mathcal{L}_0/M w.r.t. bM (Bottom).

and, the specific angular momentum reads

$$\mathcal{L}_0 = \frac{r_0 \sqrt{b^2 r_0^2 (r_0 - 2M)^2 + M(r_0 - 3M)}}{r_0 - 3M} - \frac{bM r_0^2}{r_0 - 3M}. \quad (33)$$

In an innermost stable circular orbit the second derivative of the potential should necessarily vanish, which gives us

the following condition

$$b^2 r_{ISCO}^3 (5r_{ISCO} - 4M) - 4b \mathcal{L}_0 M r_{ISCO} - \mathcal{L}_0^2 + 2M r_{ISCO} = 0. \quad (34)$$

From equation (34) we have found that the magnetic field always tries to sharpen the boundaries of the ISCO region. As the magnetic parameter b approaches ∞ , the

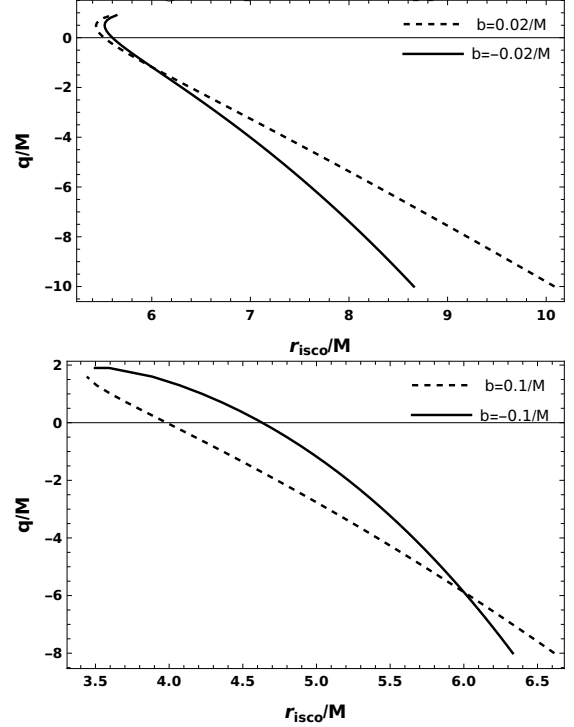


FIG. 4. The r_{ISCO}/M versus q/M for selected values of b for weak (Top) and strong magnetic field (Bottom).

r_{ISCO} approaches $2M$ and for $-\infty$ the r_{ISCO} approaches the value $(\sqrt{13} + 5)M/2$. Fig.3 shows the behavior of the radius, the specific energy, and the specific angular momentum w.r.t. the charge q/M .

Now, we simultaneously switch both the charge parameter $q \neq 0$ and the magnetic parameter $b \neq 0$. Applying the two conditions $V(r) = \mathcal{E}$ and $V'(r) = 0$ for circular orbits to the effective potential (24) yields the following result

$$\mathcal{E}_0 = \frac{q}{r_0} + \sqrt{\left[1 + \left(\frac{\mathcal{L}_0}{r_0} - br_0\right)^2\right] \left(1 - \frac{2M}{r_0}\right)}. \quad (35)$$

Due to the colossal expression for specific angular momentum, we will skip writing it here. However, the condition for ISCO is as follows

$$\begin{aligned}
& b^2 r_{ISCO}^3 (5r_{ISCO} - 4M) - 4b \mathcal{L}_0 M r_{ISCO} - \mathcal{L}_0^2 + 2M r_{ISCO} \\
& - \frac{q}{r_{ISCO}} \sqrt{r_{ISCO} (r_{ISCO} - 2M) \{(\mathcal{L}_0 - b r_{ISCO}^2)^2 + r_{ISCO}^2\}} - \frac{q}{\sqrt{r_{ISCO} (r_{ISCO} - 2M) \{(\mathcal{L}_0 - b r_{ISCO}^2)^2 + r_{ISCO}^2\}}} \\
& \times \left\{ b^2 r_{ISCO}^4 (2r_{ISCO} - 3M) + 2b \mathcal{L}_0 r_{ISCO}^2 (M - r_{ISCO}) + \mathcal{L}_0^2 M + r_{ISCO}^2 (r_{ISCO} - M) \right\} = 0. \tag{36}
\end{aligned}$$

A clear visualization of r_{ISCO} when both q and b are nonzero can be better perceived by the graphical comparison of r_{ISCO}/M w.r.t. q/M for different values of b .

We can readily conceive from the plots given in figure 4 that at the inflection manifolds the magnetic field sharpens the orbital boundaries of circular orbits. The magnetic fields have three major effects on the radius of ISCO: First, it brings the radius of ISCO closer to the coordinate singularity or the event horizon.

In all cases where the magnetic parameter $b \neq 0$ r_{ISCO} is always finite. Second, it makes the maximum value of the charge always greater than M for which r_{ISCO} exists. And third, it can create two concurrent ISCO's when $b < 0$. All these effects become more evident as the magnitude of the magnetic field parameter increases; see figure 4.

III. KERR BLACK HOLE

The Schwarzschild black hole, as discussed in section II, is non-rotating, a heuristic solution of Einstein's field equation for rotating body of mass M and specific angular momentum a was derived by R. Kerr [19]. The Kerr metric is the most unique stationary axisymmetric vacuum solution (Carter-Robinson theorem), just as the Schwarzschild metric is the most static vacuum solution (Israel's theorem).

In Boyer Lindquist coordinates

$$\Delta = r^2 - 2Mr + a^2 \quad \text{and} \quad \rho^2 = r^2 + a^2 \cos^2 \theta, \tag{37}$$

since $g_{\mu\nu}(r, \theta)$ is symmetric, so $g_{t\phi} = g_{\phi t}$. The squared line element of the Kerr metric is:

$$\begin{aligned}
ds^2 = & - \left(\frac{\Delta - a^2 \sin^2 \theta}{\rho^2} \right) dt^2 - \frac{4aMr \sin^2 \theta}{\rho^2} dt d\phi \\
& + \frac{\Gamma \sin^2 \theta}{\rho^2} d\phi^2 + \frac{\rho^2}{\Delta} dr^2 + \rho^2 d\theta^2 \tag{38}
\end{aligned}$$

We will study the circular orbits of neutral particles and the innermost stable circular orbits of neutral and charged particles in the Kerr field, as we have done in section II for Schwarzschild black hole.

A. Circular orbits of gravitating neutral particles in Kerr field

In this section, we discuss how particles orbit around the Kerr black hole in the absence of electric and magnetic fields. An interesting sub-manifold to evaluate the quadrature is the equatorial sub-manifold. For an equatorial sub-manifold:

$$\theta = \frac{\pi}{2}, \quad \dot{\theta} = 0, \quad \rho^2 = r^2 \quad \text{and} \quad \Gamma = (r^2 + a^2)^2 - a^2 \Delta.$$

Hereinafter Γ is the Boyer Lindquist coordinate for the equatorial manifold. The squared line element of the Kerr spacetime in the equatorial sub-manifold is

$$ds^2 = - \left(\frac{\Delta - a^2}{r^2} \right) dt^2 - \frac{4aM}{r^2} dt d\phi + \frac{\Gamma}{r^2} d\phi^2 + \frac{r^2}{\Delta} dr^2 + r^2 d\theta^2. \tag{39}$$

The Kerr metric, just like the Schwarzschild metric, due to its temporal and azimuthal symmetry, allows two killing vectors

$$\psi^\mu = \left(\frac{\partial}{\partial t} \right)^\mu \quad \text{and} \quad \chi^\mu = \left(\frac{\partial}{\partial \phi} \right)^\mu. \tag{40}$$

The corresponding conserved quantities are the energy and the angular momentum, respectively. If the four-velocity of a test particle in the Kerr background is u^μ , then, the contraction of four-velocity is $g_{ab} u^a u^b = -k$ with $k = 1$ for timelike events and 0 for lightlike events.

The specific energy and specific angular momentum take the form:

$$\mathcal{E} = -u^\mu \psi_\mu = -g_{\mu\nu} u^\mu u^\nu \quad \text{and} \quad \mathcal{L} = u^\mu \chi_\mu. \tag{41}$$

The component-wise and explicit forms of the specific energy and specific angular momentum are

$$\mathcal{E} = \left(\frac{\Delta - a^2}{r^2} \right) \dot{t} + \frac{2Ma}{r} \dot{\phi} \quad \text{and} \quad \mathcal{L} = \frac{-2Ma}{r} \dot{t} + \frac{\Gamma}{r^2} \dot{\phi}. \tag{42}$$

The expanded form of $g_{ab} u^a u^b = -k$ is

$$\left(\frac{\Delta - a^2}{2} \right) \dot{t}^2 + \frac{4aM}{r} \dot{t} \dot{\phi} - \frac{\Gamma}{r^2} \dot{\phi}^2 - \frac{r^2}{\Delta} \dot{r}^2 = k. \tag{43}$$

The radial equation of the equatorial sub-manifold can be written as the function of \mathcal{E} and \mathcal{L} instead of \dot{t} and $\dot{\phi}$, using equations (42) to write \dot{t} and $\dot{\phi}$ as functions of \mathcal{E} and \mathcal{L} , we get

$$\dot{r}^2 = \frac{r^2}{\Delta - a^2} \left[\mathcal{E} - \frac{2Mar \mathcal{L} (\Delta - a^2) + 4M^2 a^2 r^2 \mathcal{E}}{\Gamma (\Delta - a^2) + M^2 a^2 r^2} \right] \tag{44}$$

and

$$\dot{\phi} = \left[\frac{\mathcal{L}(\Delta - a^2)r^2 + 2Mar^3\mathcal{E}}{\Gamma(\Delta - a^2) + 4a^2M^2r^2} \right]. \quad (45)$$

Now, substituting (44) and (45) in (43), we get

$$\begin{aligned} \dot{r}^2 = & \left\{ -k + \left[\frac{r^2}{\Delta - a^2} \right] \left[\mathcal{E} - \frac{\mathcal{L}(\Delta - a^2)2Mar + 4M^2r^2a^2\mathcal{E}}{\Gamma(\Delta - a^2) + 4M^2a^2r^2} \right]^2 - \frac{\Gamma}{r^2} \left[\frac{\mathcal{L}(\Delta - a^2)r^2 + 2Mar^3\mathcal{E}}{\Gamma(\Delta - a^2) + 4a^2M^2r^2} \right]^2 \right. \\ & \left. + \frac{4aMr}{(\Delta - a^2)} \left[\mathcal{E} - \frac{\mathcal{L}(\Delta - a^2)2Mar + 4M^2r^2a^2\mathcal{E}}{\Gamma(\Delta - a^2) + 4M^2a^2r^2} \right] \left[\frac{\mathcal{L}(\Delta - a^2)r^2 + 2Mar^3\mathcal{E}}{\Gamma(\Delta - a^2) + 4M^2a^2r^2} \right] \right\} \left/ \frac{r^2}{\Delta} \right. \end{aligned} \quad (46)$$

An immediate verification of this radial equation can be performed using the fact that when the Kerr parameter a is set to 0, the Kerr metric reduces to the Schwarzschild metric. Therefore, $\Delta = r^2 - 2Mr$ and $\Gamma = r^4$ and this reparametrization for timelike geodesics ($k = 1$) reduce the equation (46) into

$$\dot{r}^2 + \left(1 - \frac{2M}{r}\right) \left(1 + \frac{\mathcal{L}^2}{r^2}\right) = \mathcal{E}^2, \quad (47)$$

which is same as for the Schwarzschild black hole, see

equation (5). The radial dynamical equation (46), therefore, is more general and applicable to all the test particles outside the ergo-sphere of the Kerr black hole. This equation also assumes two non extraneous solutions, i.e., positive and negative solutions. The analytic solution of this differential equation is very difficult. After a lot of algebraic work, we found the solution of (46) for a timelike geodesic as

$$\dot{r}_{\pm} = \pm \sqrt{\frac{\mathcal{E}^2 (a^2(2M + r) + r^3) - a^2r - 4a\mathcal{E}\mathcal{L}M + (\mathcal{L}^2 + r^2)(2M - r)}{r^3}}. \quad (48)$$

We can validate equation (46) simply by squaring equation (48) and setting $a = 0$, which reduces equation (48) to equation (5), as expected.

For the null geodesics (or lightlike events for which $k = 0$), the solution takes the form of

$$\dot{r}_{\pm} = \pm \sqrt{\frac{\mathcal{E}^2 (a^2(2M + r) + r^3) - 4a\mathcal{E}\mathcal{L}M + \mathcal{L}^2(2M - r)}{r^3}}. \quad (49)$$

By squaring equations (49) and setting $a = 0$, the result turns out to be Equation 6.3.29 of Wald [3], which reads the effective potential as

$$V_{eff} = \frac{\mathcal{L}^2}{2r^3}(r - 2M). \quad (50)$$

Just like the Schwarzschild metric, Kerr black holes also show the phenomenon of innermost stable circular orbits. We can convert equation (48) into classical quadrature by squaring

$$\dot{r}^2 r^3 = \mathcal{E}^2 (a^2(2M + r) + r^3) - a^2r - 4a\mathcal{E}\mathcal{L}M + (\mathcal{L}^2 + r^2)(2M - r), \quad (51)$$

and upon simplification, the quadrature of a Kerr metric in an equatorial sub-manifold takes the form as

$$\frac{1}{2}\dot{r}^2 - \frac{M}{r} + \frac{\mathcal{L}^2}{2r^2} + \frac{1}{2}(1 - \mathcal{E}^2) \left(1 + \frac{a^2}{r^2}\right) - \frac{M}{r^3}(\mathcal{L} - a\mathcal{E})^2 = 0. \quad (52)$$

The relativistically effective potential, thus, is given as

$$V_{eff}(r, \mathcal{E}, \mathcal{L}) = -\frac{M}{r} + \frac{\mathcal{L}^2}{2r^2} + \frac{1}{2}(1 - \mathcal{E}^2) \left(1 + \frac{a^2}{r^2}\right) - \frac{M}{r^3}(\mathcal{L} - a\mathcal{E})^2. \quad (53)$$

The variation of the effective potential of the Kerr black hole with respect to r for different values of charge a is shown in figure 5.

The condition for any test particles to execute circular motion in the Kerr field is the simultaneous solution of $V_{eff} = 0$ and $V'_{eff} = 0$. Now, as

$$V'_{eff} = -\frac{a^2(1 - \mathcal{E}^2)}{r^3} + \frac{3M(\mathcal{L} - a\mathcal{E})^2}{r^4} - \frac{\mathcal{L}^2}{r^3} + \frac{M}{r^2} = 0, \quad (54)$$

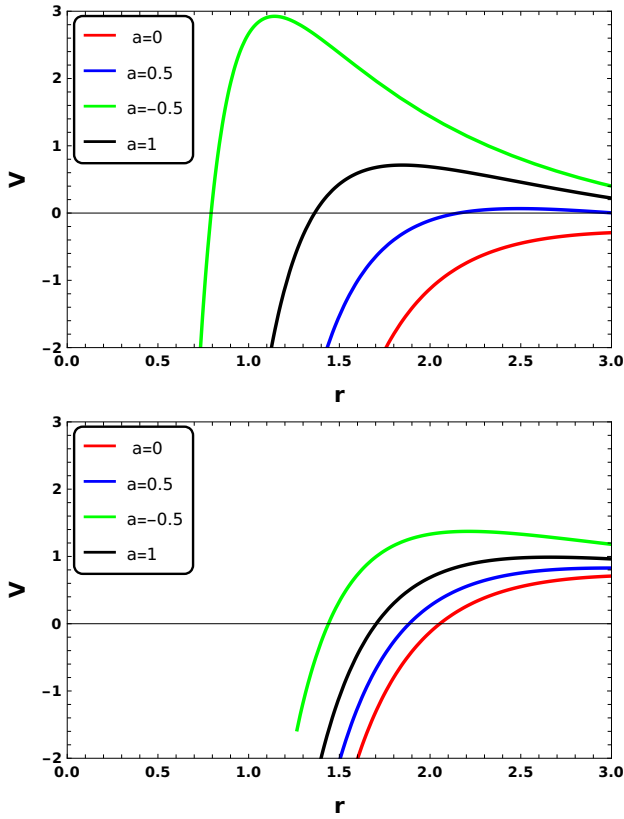


FIG. 5. Variation of effective potential of Kerr black hole with r for different values of a with $\mathcal{E} = 0.5$ and (Top) and $\mathcal{E} = 1$ (Bottom).

and the roots of this equation are

$$r_{\pm} = \frac{\mathcal{L}^2 + a^2 - a^2\mathcal{E}^2}{2M} \pm \frac{\sqrt{(a^2\mathcal{E}^2 - a^2 - \mathcal{L}^2)^2 - 12M^2(\mathcal{L} - a\mathcal{E})^2}}{2M}. \quad (55)$$

Setting $a = 0$ results in (8), as expected, validates (55). Now, if $(a^2\mathcal{E}^2 - a^2 - \mathcal{L}^2)^2 < 12M^2(\mathcal{L} - a\mathcal{E})^2$ then there are no maxima or minima of $V(r, \mathcal{E}, \mathcal{L})$ which means the particle is trapped and the information is lost. However, the physically most important case is when $(a^2\mathcal{E}^2 - a^2 - \mathcal{L}^2)^2 > 12M^2(\mathcal{L} - a\mathcal{E})^2$. It has been verified that r_+ is a minima of $V(r, \mathcal{E}, \mathcal{L})$ and r_- is a maxima. The use of equation (55) in equations (53) and (54) produces the expressions for specific energy and specific angular momentum, respectively, as

$$\mathcal{E}_0 = \frac{(r_0 - M)r_0 + (r_0^2 + a^2 - 2Mr_0)}{2r_0\sqrt{r_0^2 + a^2 - 2Mr_0}} \quad (56)$$

and

$$\mathcal{L}_0 = \frac{r_0^2 + a^2}{a}\mathcal{E}_0 - \frac{a\sqrt{r_0^2 + a^2 - 2Mr_0}}{r_0}. \quad (57)$$

Now the condition for Innermost stable circular orbits to exist necessitates the second derivative of effective potential (53) to vanish, that is,

$$a^2 (\mathcal{E}_0^2(3M + r_0) - r_0) - 6a\mathcal{L}_0M\mathcal{E}_0 + \mathcal{L}_0^2(3M - r_0) + Mr_0^2 = 0. \quad (58)$$

The sufficient and necessary condition for the radius of orbit to be equal to r_{ISCO} is algebraically obtained by putting equations (56) and (57) in equation (58), which gives

$$r_{ISCO}(r_{ISCO} - 6M) + 8a\sqrt{Mr_{ISCO}} - 3a^2 = 0. \quad (59)$$

The energy and angular momentum of a test particle in an ISCO of Kerr black hole are respectively

$$\mathcal{E}_{ISCO} = \sqrt{1 - \frac{2M}{3r_{ISCO}}}$$

and

$$\mathcal{L}_{ISCO} = \sqrt{\frac{2M}{3r_{ISCO}}(3r_{ISCO}^2 - a^2)}. \quad (60)$$

Here, it should be noted that r_{ISCO} lies in the interval $[M, 9M]$. The value of \mathcal{E}_{ISCO} when $r_{ISCO} = 2M$ is $\sqrt{2}/\sqrt{3}$. A particle entering the ISCO will release an energy of up to $1 - \sqrt{2}/\sqrt{3} \approx 18.3\%$ of its rest energy.

B. ISCO of charged particles in Kerr black hole

After discussing the relativistic properties of neutral particles in the Kerr field, we are in a position to discuss the electrodynamic properties of charged particles in the Kerr field. As already stated in equation (40), the Kerr metric allows for two symmetries —temporal and azimuthal. We can use these two symmetries to construct the relativistic electromagnetic four potential:

$$A^\mu = \left(aB - \frac{Q}{2M}\right)\psi_{(t)}^\mu + \frac{B}{2}\psi_{(\phi)}^\mu, \quad (61)$$

around a charged Kerr black hole immersed in an axisymmetric magnetic field, see [12]. Here, Q is the black hole charge and B is the axisymmetric magnetic field strength. Now, by an already followed procedure in the Schwarzschild field, we find, respectively, the specific energy and specific angular momentum of a charged particle in the Kerr field as

$$\begin{aligned} \mathcal{E} &= -\frac{p_\mu\psi_{(t)}^\mu}{m} \\ &= \frac{q - 4Mab}{r} + \left(1 - \frac{2M}{r}\right)i + \frac{2Ma}{r}(b + \phi) \end{aligned} \quad (62)$$

and

$$\mathcal{L} = \frac{p_\mu \psi^\mu_{(\phi)}}{m} = \left[\frac{a(q - 4Mab)}{r} - \frac{2Ma}{r} \dot{t} + \frac{r^3 + a^2 r - 2Ma^2}{r} (b + \dot{\phi}) \right]. \quad (63)$$

$$r^3 \dot{r}^2 = \left(\frac{q - 2abM}{r} - \mathcal{E} \right)^2 \left\{ r^3 + ra^2 - 2Ma^2 \right\} + 4Ma \left(\frac{q - 2abM}{r} - \mathcal{E} \right) \times \left[\frac{(q - 4abM)a}{r} - b \left\{ \frac{r^3 + ra^2 - 2Ma^2}{r} \right\} + \mathcal{L} \right] - r \left[\left(1 - \frac{2M}{r} \right) \times \left\{ r^2 + \left(\frac{(q - 4abM)a}{r} - b \frac{r^3 + ra^2 - 2Ma^2}{r} + \mathcal{L} \right)^2 \right\} + a^2 \right]. \quad (64)$$

The weak field approximation for Kerr black holes also breaks down when the electric and magnetic fields near black holes create curvature comparable to the black holes mass near the event horizon, as already stated in equation (25), see [7]. Due to the complexity of the above equation (64), we cannot write the explicit expressions for the first and second derivatives of equation (64). We will study the behavior of charges around weakly charged and weakly magnetized black holes graphically, rather than algebraically.

We will first explain the electric and magnetic effects separately. If we switch off the magnetic field, i.e., $b = 0$, the problem is still extremely complex to solve by any analytical method. We have used numerical simulations to study the phenomenon graphically.

The graphs shown above (Figure 6) were plotted for the positive values of the charge parameter, which means when the test particle and the black hole have the same charge. Again we will plot the graphs (Figure 7) for the negative values of the charge parameter i.e., when the test particle and the black hole are of opposite charge.

From both figures it can be readily conceived that with an increase in the magnitude of the charge parameter q the radius of ISCO increases. An enormously important point that we obtained is that when $q = M$ then the ISCO falls in the interval $[M, \infty]$ with $\mathcal{E}_{ISCO} = 1$ and $\mathcal{L}_{ISCO} = M$ for all values of r . This perplexing conclusion tells us that a charged particle at infinity can be entangled to a Kerr black hole for which $q = M$. Next, we study the variation of radius r_{ISCO}/M , energy \mathcal{E}_{ISCO} and angular momentum \mathcal{L}_{ISCO}/M with the Kerr parameter a/M for different values of the magnetic parameter b by switching off the charge parameter q , i.e., $q = 0$.

The graphs shown above (Figure 8) were plotted for the positive values of the magnetic parameter, which means when the charge of a test particle and the magnetic field of the black hole have the same sign. Now, we plot the graphs (Figure 9) for the negative values of the magnetic parameter i.e., when the charge of a test particle and the magnetic field of the black hole are of opposite sign.

Here, again, we have parameterized $q = eQ/m$ and $b = eB/2m$. Similarly, as in the Schwarzschild black hole, we can construct the radial quadrature of the Kerr field as

Lastly, we can check the variation of radius r_{ISCO}/M , energy \mathcal{E}_{ISCO} and angular momentum \mathcal{L}_{ISCO}/M with the Kerr parameter a/M for different values of the magnetic parameter by switching on the magnetic parameter b , i.e., $b \neq 0$.

The graphs shown above (Figure 10) were plotted for the positive values of the charge parameter in the presence of a magnetic field, which means when the test particle and the black hole have the same charge. Again, we plot the graphs (Figure 11) for the negative values of the charge parameter in presence of magnetic field, i.e., when the test particle and the black hole are of opposite charge.

IV. REISSNER-NORDSTRÖM BLACK HOLE

The next important class of black holes is the famous Reissner-Nordström. These are the spherically symmetric non-rotating charged black holes. The spin parameter for these black holes vanishes, i.e., $a = 0$, but they have the charge, say e . The geometry of Reissner-Nordström suggests that the true physical singularity no longer has a ring structure. The metric of the Reissner-Nordström black hole in the spherical polar coordinates has the form [20, 21]:

$$ds^2 = -\frac{\Delta}{r^2} dt^2 + \frac{r^2}{\Delta} dr^2 + r^2 d\theta^2 + r^2 \sin^2 \theta d\phi^2. \quad (65)$$

We can make a Boyer-Lindquist-like substitution to enhance the reduction: $\Delta = r^2 + e^2 - 2Mr$. As long as the charge distribution of Reissner-Nordström black hole is spherically symmetric, Birkhoff's theorem is applicable. The physical boundaries of the metric are determined by setting $\Delta = 0$, which implies

$$r_{\pm} = M \pm \sqrt{M^2 - e^2}.$$

The event horizons for r_{\pm} exist only when $M^2 \geq e^2$. Throughout the discussion of Reissner-Nordström black holes, we will assume this condition to hold.

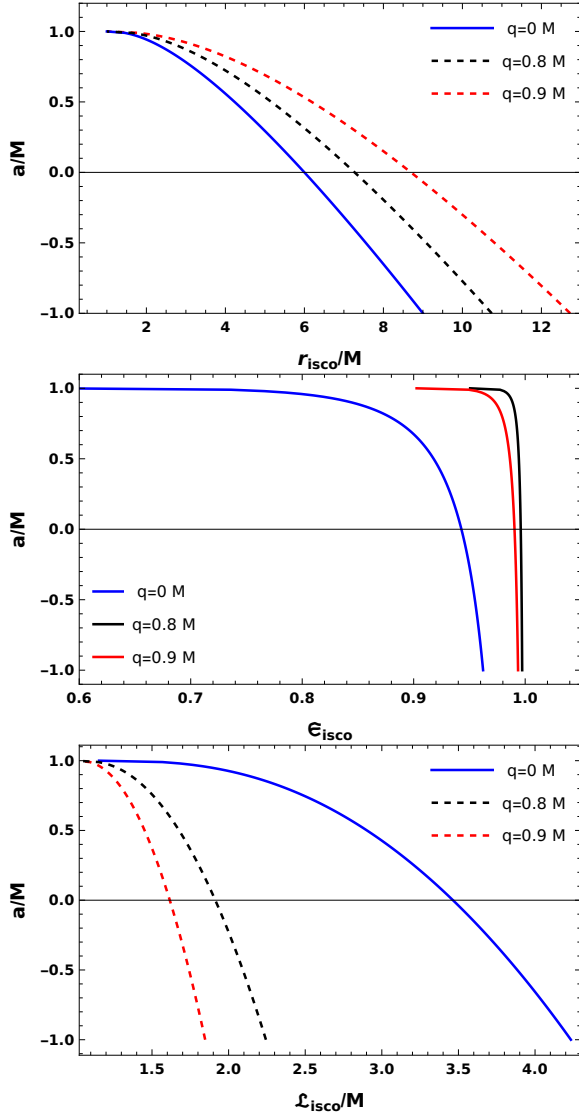


FIG. 6. Variation of radius r_{ISCO}/M (Top), energy \mathcal{E}_{ISCO} (Center) and angular momentum \mathcal{L}_{ISCO}/M (Bottom) with a/M for positive values of charge parameter q .

A. Circular orbits of gravitating neutral particles in Reissner-Nordström black hole

In this section we discuss the circular orbits of neutral particles in the equatorial sub-manifold of black hole. We know, in an equatorial region: $\theta = \frac{\pi}{2}$ and $\dot{\theta} = 0$. The Reissner-Nordström metric, ditto as Kerr metric, due to its temporal and azimuthal symmetry, allows two killing vectors

$$\psi^\mu = \left(\frac{\partial}{\partial t} \right)^\mu \quad \text{and} \quad \chi^\mu = \left(\frac{\partial}{\partial \phi} \right)^\mu.$$

The corresponding conserved quantities are the energy and the angular momentum, respectively. If the four-velocity of a test particle in the gravitational background is u^μ . Then, the contraction of the four-velocity is

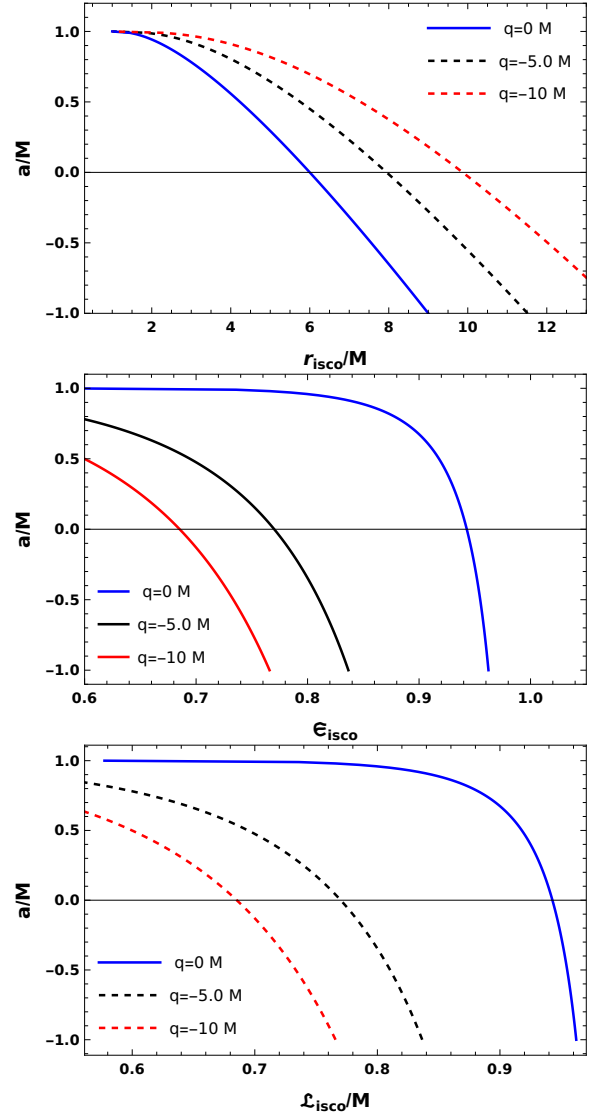


FIG. 7. Variation of radius r_{ISCO}/M (Top), energy \mathcal{E}_{ISCO} (Center) and angular momentum \mathcal{L}_{ISCO}/M (Bottom) with a/M for negative values of charge parameter q .

$g_{ab}u^a u^b = -k$, with $k = 1$ for timelike events and $k = 0$ for lightlike events.

The specific energy and specific angular momentum, thus, take the following forms:

$$\mathcal{E} = -u^\mu \psi_\mu = -g_{\mu\nu} u^\mu u^\nu \quad \text{and} \quad \mathcal{L} = u^\mu \chi_\mu.$$

These tensorial equations help us evaluate i and $\dot{\phi}$, these are

$$i = \frac{r^2}{\Delta} \mathcal{E} \quad \text{and} \quad \dot{\phi} = \frac{\mathcal{L}}{r^2} \quad (66)$$

The radial dynamical variable equation of the equatorial sub-manifold is

$$g_{tt}u^t u^t + g_{rr}u^r u^r + g_{\theta\theta}u^\theta u^\theta + g_{\phi\phi}u^\phi u^\phi = -k. \quad (67)$$

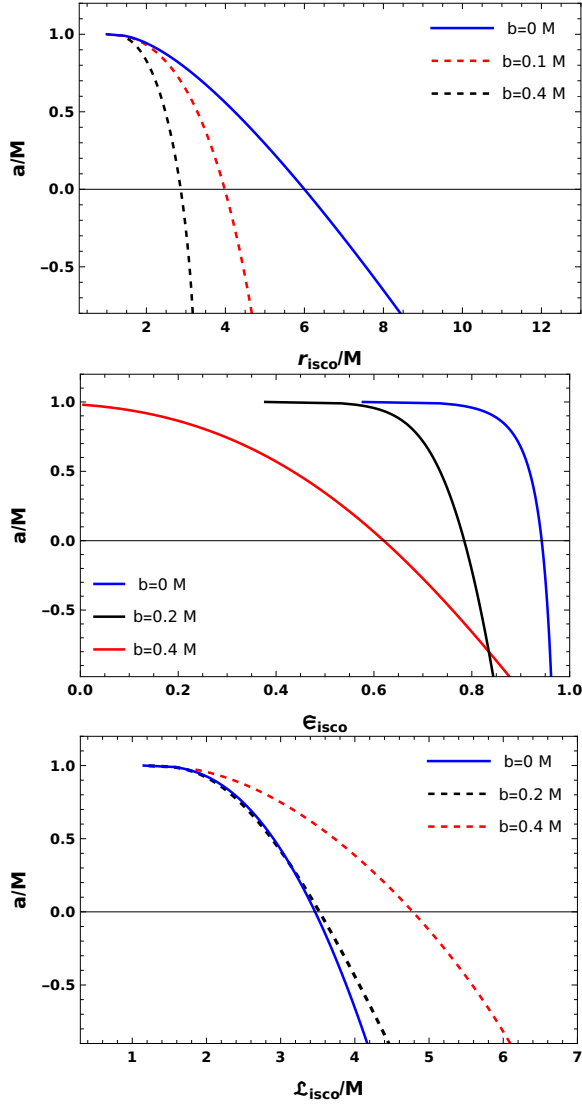


FIG. 8. Variation of r_{ISCO}/M (Top), \mathcal{E}_{ISCO} (Center) and \mathcal{L}_{ISCO}/M (Bottom) with Kerr parameter a/M for positive values of magnetic parameter b .

Now using equations (66) in equation (67), we get the quadrature of the Reissner-Nordström black hole in the equatorial sub-manifold as

$$\frac{1}{2}\dot{r}^2 + \frac{1}{2}\left(k + \frac{\mathcal{L}^2}{r^2}\right)\left[1 - \frac{2M}{r} + \frac{e^2}{r^2}\right] = \frac{1}{2}\mathcal{E}^2. \quad (68)$$

The relativistically effective potential as a function of \mathcal{L} , r and e is

$$V_{eff} = \frac{1}{2}\left(k + \frac{\mathcal{L}^2}{r^2}\right)\left[1 - \frac{2M}{r} + \frac{e^2}{r^2}\right]. \quad (69)$$

With no surprise, if we set $e = 0$ then V_{eff} reduces to equation (6) and if we put $k = 0$ it reduces to equation 6.3.29 of Wald [3].

The graphical representation of the effective potential of the Reissner-Nordström black hole w.r.t. r for different

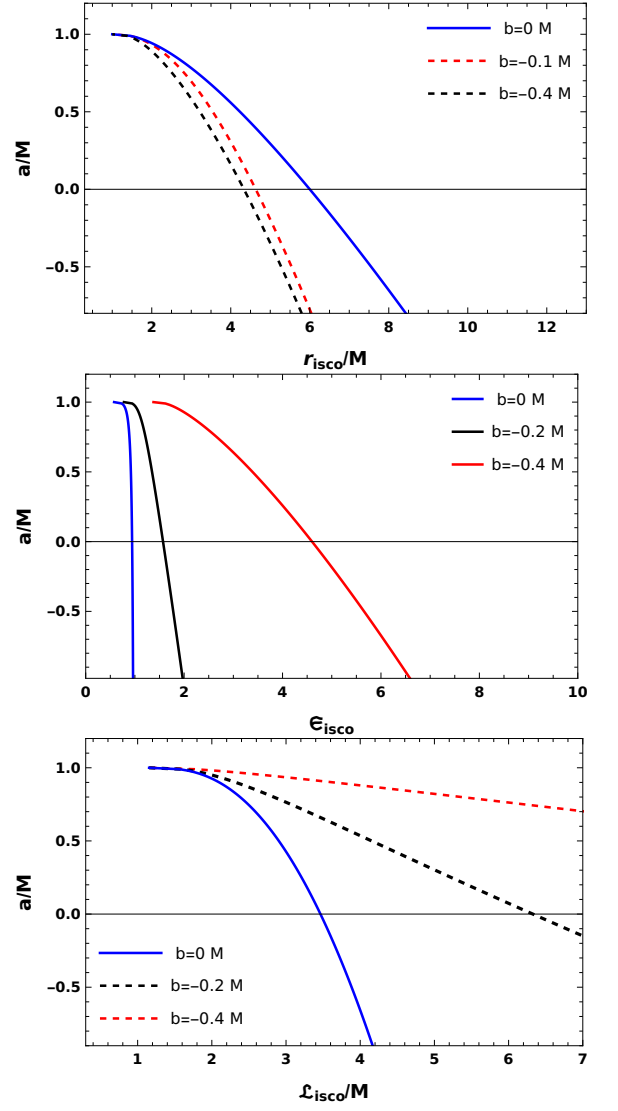


FIG. 9. Variation of r_{ISCO}/M (Top), \mathcal{E}_{ISCO} (Center) and \mathcal{L}_{ISCO}/M (Bottom) with Kerr parameter a/M for negative values of magnetic parameter b .

values of charge e is as shown in Figure 12. We see that the radius of circular orbits decreases with increase in black hole charge for the same effective potential. For a test particle to perform circular motion, both V_{eff} and its first derivative with respect to r must be zero. That is,

$$V'_{eff} = \frac{kM}{r^2} - \frac{ke^2}{r^3} - \frac{\mathcal{L}^2}{r^3} + \frac{3\mathcal{L}^2M}{r^4} - \frac{2e^2\mathcal{L}^2}{r^5} = 0$$

and the roots of this equation are

$$r = \frac{\mathcal{L}^2 + e^2}{3M} + \frac{\{P + \sqrt{Q}\}}{3(2)^{\frac{1}{3}}M} + \frac{2^{\frac{1}{3}}\{9\mathcal{L}^2M^2 - (\mathcal{L}^2 + e^2)^2\}}{3M\{P + \sqrt{Q}\}}, \quad (70)$$

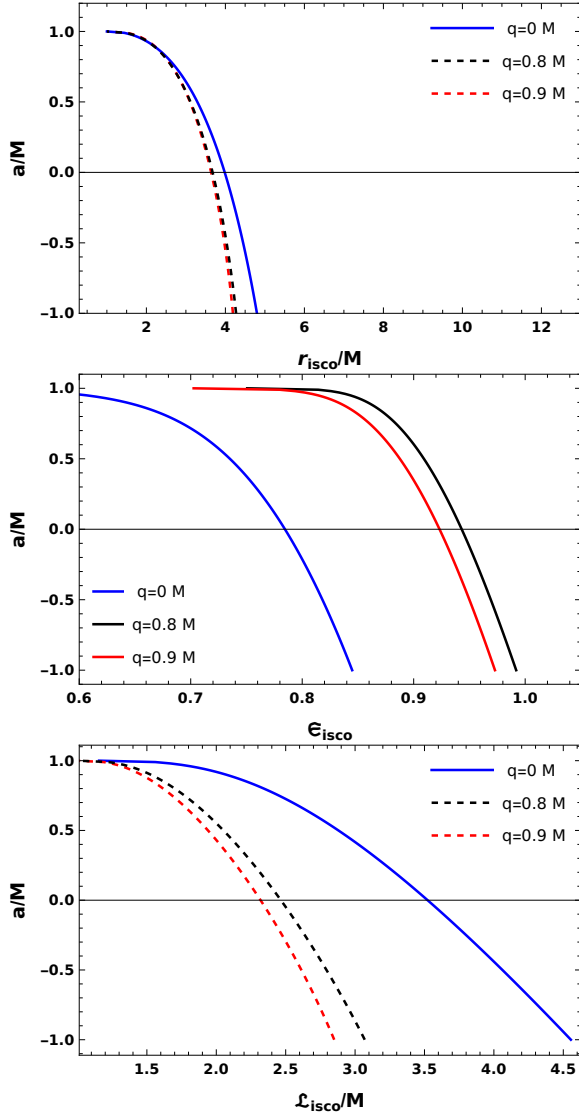


FIG. 10. Variation of r_{ISCO}/M (top), \mathcal{E}_{ISCO} (Center) and \mathcal{L}_{ISCO}/M (bottom) with Kerr parameter a/M for positive values of charge parameter q with $b = 0.1/M$.

here we have defined new functions P and Q , respectively, as

$$P = \left[2\mathcal{L}^6 - 27\mathcal{L}^4 M^2 + 6\mathcal{L}^4 e^2 + 27\mathcal{L}^2 M^2 e^2 + 6\mathcal{L}^2 e^4 + 2e^6 \right] \quad (71)$$

and

$$Q = \left[\left\{ 2\mathcal{L}^6 - 27\mathcal{L}^4 M^2 + 6\mathcal{L}^4 e^2 + 27\mathcal{L}^2 M^2 e^2 + 6\mathcal{L}^2 e^4 + 2e^6 \right\}^2 + 4 \left\{ 9\mathcal{L}^2 M^2 - (\mathcal{L}^2 + e^2)^2 \right\}^3 \right]^{\frac{1}{3}} \quad (72)$$

The sufficient and necessary condition to be satisfied by Q is $M^2 > e^2$. For a particle to execute circular motion in the Reissner-Nordstrom field, the conditions to

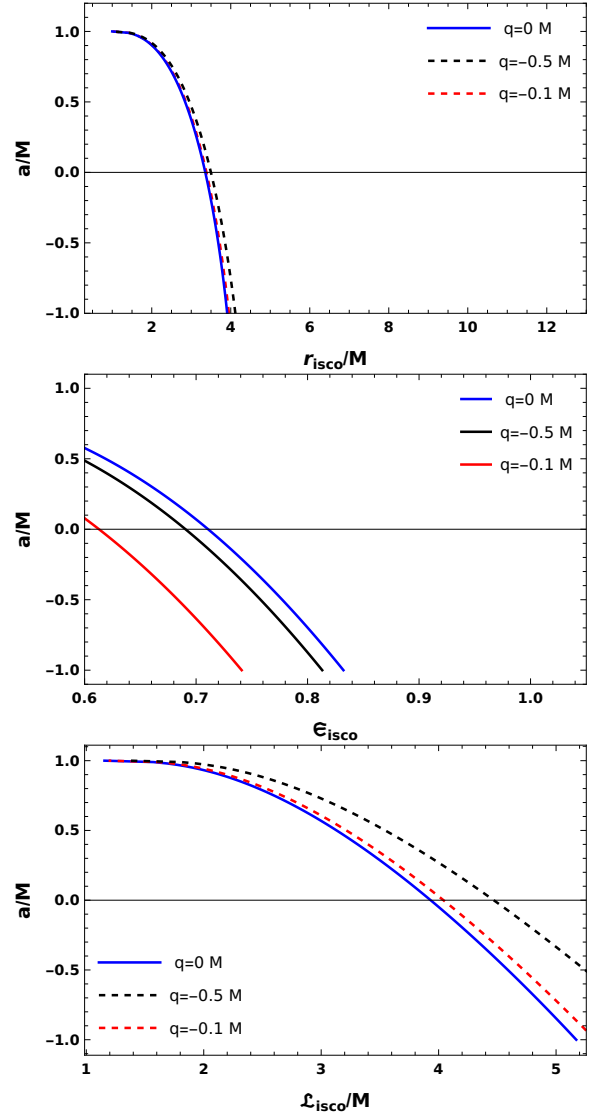


FIG. 11. Variation of r_{ISCO}/M (top), \mathcal{E}_{ISCO} (Center) and \mathcal{L}_{ISCO}/M (bottom) with Kerr parameter a/M for negative values of charge parameter q with $b = 0.2/M$.

be satisfied are

$$\mathcal{E}^2 = V_{eff}(r) \quad \text{and} \quad V'_{eff}(r) = 0.$$

For a timelike geodesic ($k = 1$), the energy for a massive particles is

$$\frac{\mathcal{E}^2}{2} = \frac{1}{2} \left(1 + \frac{\mathcal{L}^2}{r^2} \right) \left[1 - \frac{2M}{r} + \frac{e^2}{r^2} \right] = V_{eff}. \quad (73)$$

From $V'_{eff}(r) = 0$ and using \mathcal{L}^2 in equation (73), we can easily check

$$\mathcal{L} = \sqrt{\frac{Mr^3 - e^2 r^2}{r^2 - 3Mr + 2e^2}} \quad (74)$$

and

$$\mathcal{E} = \sqrt{\frac{1}{r^2} \frac{(r^2 - 2Mr + e^2)^2}{r^2 - 3Mr + 2e^2}}. \quad (75)$$

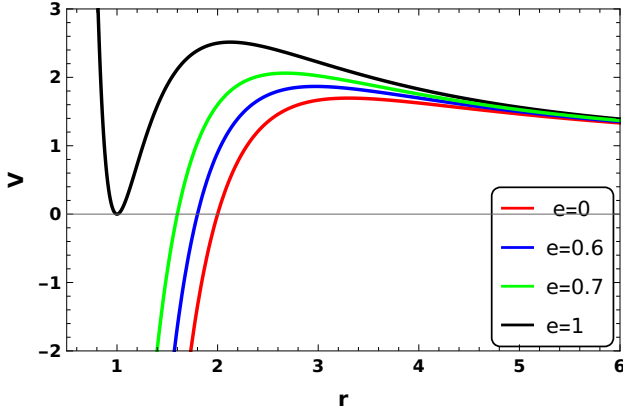


FIG. 12. Variation of effective potential of Reissner-Nordström blackhole with r for different values of e .

Reduction of Reissner-Nordström metric to Schwarzschild metric can perfectly convert equations (74) and (75) into equations (11). The condition for Reissner-Nordström black hole to have ISCO necessitates that the second derivative of $V_{eff}(r)$ should also vanish, i.e.,

$$-\frac{2M}{r^3} + \frac{3e^2}{r^4} + \frac{3\mathcal{L}^2}{r^4} - \frac{12\mathcal{L}^2 M}{r^5} + \frac{10e^2 \mathcal{L}^2}{r^6} = 0. \quad (76)$$

The roots of equation (76) that we call r_{ISCO} , with condition $M^2 \geq e^2$, were found as

$$r_{ISCO} = 2M + \frac{4M^3 - 3Me^2}{\{8M^6 - 9M^4e^2 + 2M^2e^4 + \sqrt{W}\}^{\frac{1}{3}}} + \frac{\{8M^6 - 9M^4e^2 + 2M^2e^4 + \sqrt{W}\}^{\frac{1}{3}}}{M} \quad (77)$$

where we have defined a new function,

$$W = 5M^8e^4 - 9M^6e^6 + 4M^4e^8. \quad (78)$$

We can find the specific energy and the specific angular momentum in the ISCO region by invoking equation (77) in equations (74) and (75). However, skipping writing the explicit forms due to their complex and tedious forms, we will keep them in terms of r_{ISCO} as

$$\mathcal{L}_{ISCO} = \sqrt{\frac{Mr_{ISCO}^3 - e^2r_{ISCO}^2}{r_{ISCO}^2 - 3Mr_{ISCO} + 2e^2}} \quad (79)$$

$$\mathcal{E}_{ISCO} = \sqrt{\frac{1}{r_{ISCO}^2} \frac{(r_{ISCO}^2 - 2Mr_{ISCO} + e^2)^2}{r_{ISCO}^2 - 3Mr_{ISCO} + 2e^2}}. \quad (80)$$

B. ISCO of charged particles in Reissner-Nordström black hole

After discussing the relativistic kinematic properties of neutral particles in the Reissner-Nordström field, we are

in a position to discuss the electrodynamic properties of charged particles in the Reissner-Nordström field. As already stated, the Reissner-Nordström metric allows two symmetries | temporal and azimuthal. We can use these two symmetries to construct the relativistic electromagnetic four potential. Therefore, by ansatz

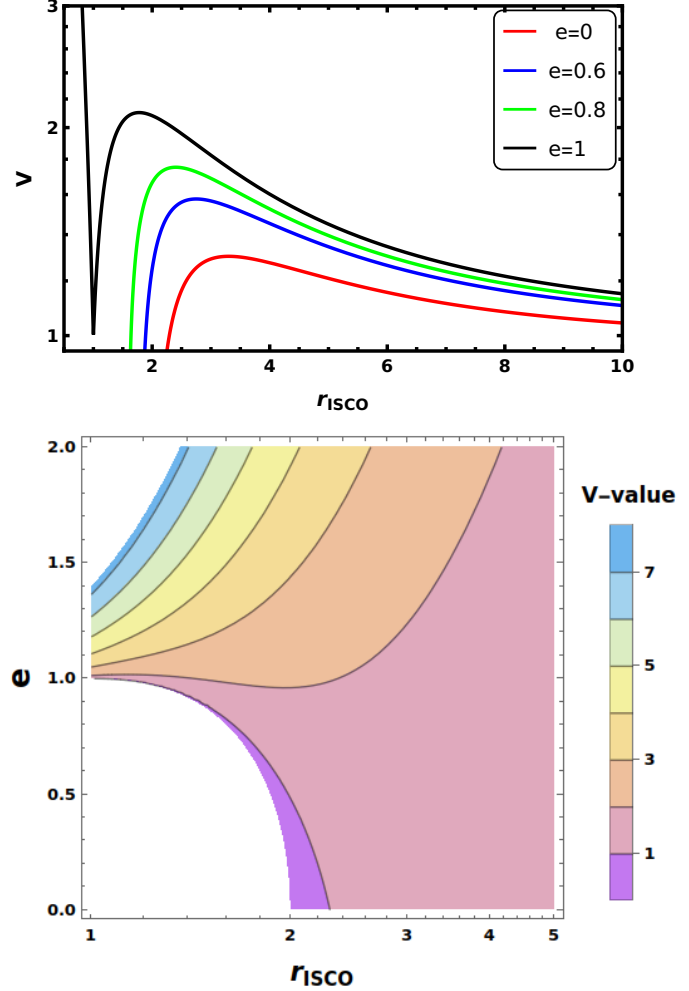


FIG. 13. Variation of r_{ISCO} with potential for different values of e (top) and charge of black hole e for different potential depths (bottom).

$$A^\mu = \frac{e}{r} - \frac{Q}{2M} \psi_{(t)}^\mu + \frac{B}{2} \psi_{(\phi)}^\mu, \quad (81)$$

where Q is the charge of the black hole and B is the axisymmetric magnetic field of the black hole. However, it must be noted that the Reissner-Nordström field has its own intrinsic charge and is denoted by e . Analogous to Schwarzschild and Kerr field we can find the radial

dynamical equation in an equatorial sub-manifold as

$$\dot{r} = \left(\frac{\mathcal{E}^2 - 1}{1 - \mathcal{E}a} \right) - \left[-\frac{1}{r} + \frac{\mathcal{L}}{r^2} - \frac{a^2 - e^2}{r^2(1 - \mathcal{E}a)} \right. \\ \left. - \left(1 - \frac{e^2}{2r} \right) \left(\mathcal{L}^2 - \frac{a^2 - e^2}{r^2(1 - \mathcal{E}a)} + \frac{a^2 - e^2}{1 - \mathcal{E}a} \right) \frac{1}{r^3} \right],$$

where, a is a charge parameter defined as eQ .

We can simplify above equation by factorizing the quadrature as

$$\dot{r} = \frac{r^4}{\mathcal{L}^2} (\mathcal{E} - V_+) (\mathcal{E} - V_-). \quad (82)$$

From this equation we can find the effective potential, by still confining our discussion to the weak field approx-

imations, as

$$V_{\pm} = \frac{e}{r} \pm \sqrt{1 - \frac{2}{r} + \frac{\mathcal{L}^2}{r^2} - \frac{2\mathcal{L}^2}{r^3} + \frac{e^2}{r^2} + \frac{\mathcal{L}^2 e^2}{r^4}}. \quad (83)$$

An easy and logical comprehension of this equation is possible by the graphical interpretation of variation of r_{ISCO} with potential for different values of e and charge of black hole e for different potential depths as shown in figure 13.

Now, by an already followed procedure, in order to find the ISCO, which is located at an inflection manifold, the first derivative and also the second derivative of effective potential ought to vanish. With these conditions, we found the necessary condition for ISCO of the charged particle in the Reissner-Nordström spacetimes as

$$\mathcal{E} \{ 3e^2 - 2r_{ISCO} \} \sqrt{9\mathcal{E}^2 r_{ISCO}^4 - 4(5\mathcal{E}^2 + 4)r_{ISCO}^3 + 12(\mathcal{E}^2 + 3)r_{ISCO}^2 - 24r_{ISCO} + 4e^2} \\ + 6\mathcal{E}^2 r_{ISCO}^3 - 3(2 + (3e^2 + 2)\mathcal{E}^2)r_{ISCO}^2 + (5\mathcal{E}^2 e^2 + 4e^2 + 2)r_{ISCO} - 6e^2 = 0. \quad (84)$$

From the plot (Figure 13) it is conspicuously clear that charged black holes enhance the stability of circular orbits, check by comparing potentials for different values of charge of black hole.

The value of a for which the minimal ISCO exists is given by the relation

$$a = 2e \sqrt{\frac{-5e^2 + 9(1 - \sqrt{1 - e^2})}{25e^2 - 9}}. \quad (85)$$

The above equation shows the electromagnetic coupling effects in the vicinity of strong gravitational fields. The highest value of r_{ISCO} for which ISCO solutions can be found when $e = 1$ is

$$r_{ISCO} = 3M.$$

V. KERR-NEWMAN BLACK HOLE

The next important class of black holes is the famous Kerr-Newman black hole. These are the spherically symmetric rotating charged black holes. The spin parameter for these black holes does not vanish, i.e., $a \neq 0$ and let the charge of the Kerr-Newman black hole be e . The geometry of Kerr-Newman suggests that the true physical singularity has a ring structure. The metric of the Kerr-Newman black hole in the spherical polar coordinates has a complex and tedious structure. In the Boyer-Lindquist

coordinates:

$$\Sigma = r^2 + a^2 \cos^2 \theta, \\ \Delta = r^2 + a^2 + e^2 - 2Mr \quad \text{and} \\ \Gamma = (a^2 + r^2)^2 - \Delta a^2 \sin^2 \theta,$$

the squared line element of the Kerr-Newman metric [22], then, is:

$$ds^2 = \frac{a^2 \sin^2 \theta - \Delta}{\Sigma} dt^2 - 2a \frac{(2Mr - e^2) \sin^2 \theta}{\Sigma} dt d\phi \\ + \frac{\Gamma}{\Sigma} \sin^2 \theta d\phi^2 + \frac{\Sigma}{\Delta} dr^2 + \Sigma d\theta^2. \quad (86)$$

The Kerr-Newman metric is the most general black hole metric as predicted by the "no-hair" conjecture.

A. Circular orbits of gravitating neutral particles in Kerr-Newman black hole

In this section circular orbits in the equatorial sub-manifold of Kerr-Newman black hole are evaluated. In the equatorial manifold $\theta = \frac{\pi}{2}$ and $\dot{\theta} = 0$. The circular orbits in the equatorial sub-manifold are interesting and very insightful.

The Kerr-Newmann metric, like other metrics, due to its temporal and azimuthal symmetry, allows two killing vectors

$$\psi^\mu = \left(\frac{\partial}{\partial t} \right)^\mu \quad \text{and} \quad \chi^\mu = \left(\frac{\partial}{\partial \phi} \right)^\mu. \quad (87)$$

As Noether's theorem necessitates two conservation laws corresponding to each symmetry. Corresponding to temporal symmetry is the conservation of specific energy \mathcal{E} and corresponding to azimuthal symmetry is the conservation of specific angular momentum \mathcal{L} . The respective quantities are:

$$\mathcal{E} = -u^\mu \zeta_\mu = -\frac{a^2 \sin^2 \theta - \Delta}{\Sigma} i + 2 \left\{ \frac{a \sin^2 \theta (2Mr - e^2)}{\Sigma} \right\} \dot{\phi} \quad (88)$$

and

$$\mathcal{L} = u^\nu \psi_\nu = 2 \left\{ \frac{a \sin^2 \theta (2Mr - e^2)}{\Sigma} \right\} i + \sin^2 \theta \left[\frac{\sin^2 \theta \left\{ (a^2 + r^2)^2 - a^2 \Delta \sin^2 \theta \right\}}{\Sigma} \right] \dot{\phi} \quad (89)$$

If the four-velocity of a test particle in the gravitational background is u^μ , then the contraction of the four-velocity is

$$g_{\mu\nu} u^\mu u^\nu = -k, \quad (90)$$

with $k = 1$ for timelike events and $k = 0$ for lightlike events. The explicit form of equation (90) in the equatorial sub-manifold is

$$\left(\frac{2Mr - r^2 - e^2}{r^2} \right) i^2 + \frac{2a}{r^2} (e^2 - 2Mr) i \dot{\phi} + \left(\frac{r^2}{r^2 + a^2 + e^2 - 2Mr} \right) \dot{r}^2 + \left(\frac{r^4 + a^2 r^2 - a^2 e^2 + 2Ma^2 r}{r^2} \right) \dot{\phi}^2 = -k. \quad (91)$$

Specific energy (\mathcal{E}) and specific angular momentum (\mathcal{L}) in the equatorial sub-manifold of Kerr-Newman space-time take the forms as

$$\mathcal{E} = \frac{r^2 - e^2 - 2Mr}{r^2} i + a \frac{2Mr - e^2}{r^2} \dot{\phi} \quad (92)$$

and

$$\mathcal{L} = a \frac{e^2 - 2Mr}{r^2} i + \frac{(r^2 + a^2)^2 - \Delta a^2}{r^2} \dot{\phi}. \quad (93)$$

In order to obtain the radial dynamical variable, equations (92) and (93) are used to obtain the expressions for

i and $\dot{\phi}$ in terms of \mathcal{E} and \mathcal{L} , and are, therefore, expressed respectively as .

$$i = \frac{r^2 (a \mathcal{L} (e^2 - 2Mr) + r^4 \mathcal{E} + a^2 \mathcal{E} (-e^2 + r(2M + r)))}{a^2 (-2e^2 r(2M + r) + 2e^4 + r^4) + r^4 (r(r - 2M) - e^2)}$$

and

$$\dot{\phi} = \frac{r^2 (-a \mathcal{E} (e^2 - 2Mr) + \mathcal{L} r (r - 2M) - \mathcal{L} e^2)}{a^2 (-2e^2 r(2M + r) + 2e^4 + r^4) + r^4 (r(r - 2M) - e^2)}$$

Now using these equations in equation (91), we get the radial dynamical equation as

$$\begin{aligned} \dot{r}^2 = & \left\{ -k + \left[\frac{r^2 + e^2 - 2Mr}{r^2} \right] \left[\frac{r^2 (a \mathcal{L} (e^2 - 2Mr) + r^4 \mathcal{E} + a^2 \mathcal{E} (-e^2 + r(2M + r)))}{a^2 (-2e^2 r(2M + r) + 2e^4 + r^4) + r^4 (r(r - 2M) - e^2)} \right]^2 + \frac{2a}{r^2} (2Mr - e^2) \right\} \times \\ & \times \left[\frac{r^2 (a \mathcal{L} (e^2 - 2Mr) + r^4 \mathcal{E} + a^2 \mathcal{E} (-e^2 + r(2M + r)))}{a^2 (-2e^2 r(2M + r) + 2e^4 + r^4) + r^4 (r(r - 2M) - e^2)} \right] \left[\frac{r^2 (-a \mathcal{E} (e^2 - 2Mr) + \mathcal{L} r (r - 2M) - \mathcal{L} e^2)}{a^2 (-2e^2 r(2M + r) + 2e^4 + r^4) + r^4 (r(r - 2M) - e^2)} \right] \\ & - \left[\frac{r^4 + a^2 r^2 - a^2 e^2 + 2Ma^2 r}{r^2} \right] \left[\frac{r^2 (-a \mathcal{E} (e^2 - 2Mr) + \mathcal{L} r (r - 2M) - \mathcal{L} e^2)}{a^2 (-2e^2 r(2M + r) + 2e^4 + r^4) + r^4 (r(r - 2M) - e^2)} \right]^2 \left/ \left[\frac{r^2}{r^2 + a^2 + e^2 - 2Mr} \right] \right\}. \quad (94) \end{aligned}$$

Verification of this radial equation can be carried out by using the fact that when the Kerr parameter $a = 0$ the Kerr-Newman metric reduces to the Reissner-Nordström metric. Therefore, this reparametrization for timelike

geodesics ($k = 1$) reduces (94) into

$$\frac{1}{2} \dot{r}^2 + \frac{1}{2} \left(k + \frac{\mathcal{L}^2}{r^2} \right) \left[1 - \frac{2M}{r} + \frac{e^2}{r^2} \right] = \frac{1}{2} \mathcal{E}^2, \quad (95)$$

which is exactly the quadrature of the Reissner-

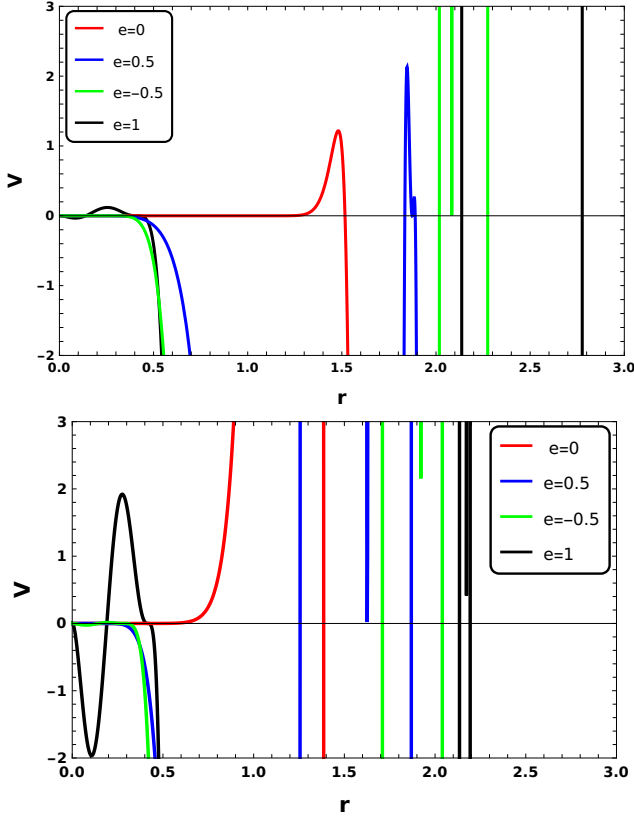


FIG. 14. Variation of effective potential of Kerr-Newman blackhole with r for different values of e with $\mathcal{E} = 1$, $a = 1$ (top) and $\mathcal{E} = 0.8$, $a = 1.5$ (bottom).

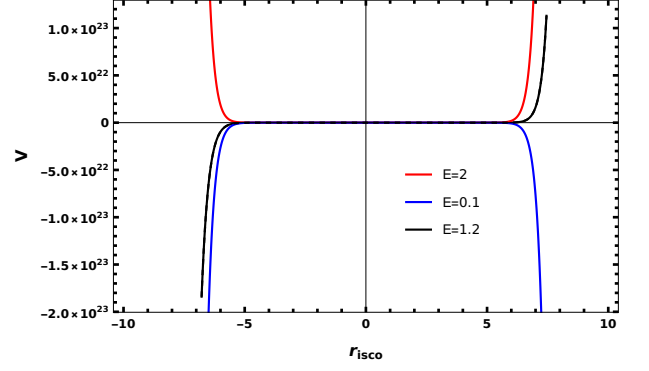


FIG. 15. The variation of potential w.r.t. r_{ISCO} for different values of energy \mathcal{E}

Nordström black hole, that is, equation (68), as expected. In the same analogy, a relatively difficult test is if we set $e = 0$ and $a \neq 0$ then equation (94) turns into equation (46), as should be. If we set both $a = 0$ and $e = 0$ which means the blackhole under consideration is charge-less and non-rotating. This parametrization converts equation (94) into equation (5), which is a Schwarzschild black hole, as it ought to be. Hence, equation (94) is the most general radial dynamical equation of a particle in the equatorial sub-manifold around a black hole. Equation (94) also assumes two solutions, i.e., positive and negative solutions. After a lot of algebraic computation, the analytic solution of this equation for timelike geodesics obtained is

$$\dot{r}_{\pm} = \pm \frac{\sqrt{\{a^2 - 2Mr + e^2 + r^2\} \{a^4 (\mathcal{E}^2 r^6 (r(2M+r) - e^2) - (-2e^2 r(2M+r) + 2e^4 + r^4)^2) + 2a^3 \mathcal{E} \mathcal{L} r^6 (e^2 - 2Mr) + a^2 r^2 (\mathcal{L}^2 (-4e^4 r(2M+r) + r^5 (2M-r) + 4e^6 + 3e^2 r^4) + \mathcal{E}^2 r^4 (-4M^2 r^2 + 4Me^2 r - e^4 + 2r^4) - 2r^2 (r(r-2M) - e^2) (-2e^2 r(2M+r) + 2e^4 + r^4)) - 2a \mathcal{E} \mathcal{L} r^6 (2Mr - e^2) (r(r-2M) + e^2) - r^6 (\mathcal{L}^2 + r^2) (r(2M-r) + e^2)^2 + \mathcal{L}^2 r^{10} (r(r-2M) + e^2)\}}{r \{a^2 (-2e^2 r(2M+r) + 2e^4 + r^4) + r^4 (r(r-2M) - e^2)\}} \quad (96)$$

This radial dynamical equation, obviously, is the most general of all the other aforementioned dynamical equations. Now, If we substitute $e = 0$, this radial equation takes the form of equation (48), as, presumably, it should

be.

Now, the most important step of this problem is to find the quadrature of Kerr-Newman black holes. We have

$$\dot{r}^2 = \frac{\{a^2 + r(r-2M) + e^2\} \{a^4 (\mathcal{E}^2 r^6 (e^2 - r(2M+r)) + (-2e^2 r(2M+r) + 2e^4 + r^4)^2) + 2a^3 \mathcal{E} \mathcal{L} r^6 (2Mr - e^2) + a^2 r^2 (\mathcal{L}^2 (4e^4 r(2M+r) + r^5 (r-2M) - 4e^6 - 3e^2 r^4) + \mathcal{E}^2 r^4 (4M^2 r^2 - 4Me^2 r + e^4 - 2r^4) + 2r^2 (r(r-2M) - e^2) (-2e^2 r(2M+r) + 2e^4 + r^4)) + 2a \mathcal{E} \mathcal{L} r^6 (2Mr - e^2) (r(r-2M) + e^2) + r^6 (\mathcal{L}^2 + r^2) (r(2M-r) + e^2)^2 - (\mathcal{E}^2 r^{10} (r(r-2M) + e^2))\}}{\{a^2 r (-2e^2 r(2M+r) + 2e^4 + r^4) + r^5 (r(r-2M) - e^2)\}^2}. \quad (97)$$

So, the relativistic effective potential as a function of

r , \mathcal{L} and \mathcal{E} of a gravitating test particle in the equatorial

sub-manifold of the Kerr-Newman field is:

$$V_{\text{eff}}(r, \mathcal{L}, \mathcal{E}) = - \frac{\{a^2 + r(r - 2M) + e^2\} \{a^4 (\mathcal{E}^2 r^6 (e^2 - r(2M + r)) + (-2e^2 r(2M + r) + 2e^4 + r^4)^2) + 2a^3 \mathcal{E} \mathcal{L} r^6 (2Mr - e^2) + a^2 r^2 (\mathcal{L}^2 (4e^4 r(2M + r) + r^5 (r - 2M) - 4e^6 - 3e^2 r^4) + \mathcal{E}^2 r^4 (4M^2 r^2 - 4Me^2 r + e^4 - 2r^4) + 2r^2 (r(r - 2M) - e^2) (-2e^2 r(2M + r) + 2e^4 + r^4)) + 2a \mathcal{E} \mathcal{L} r^6 (2Mr - e^2) (r(r - 2M) + e^2) + r^6 (\mathcal{L}^2 + r^2) (r(2M - r) + e^2)^2 - (\mathcal{E}^2 r^{10} (r(r - 2M) + e^2))\}}{2\{a^2 r (-2e^2 r(2M + r) + 2e^4 + r^4) + r^5 (r(r - 2M) - e^2)\}^2} \quad (98)$$

The graphical representation of the effective potential of the Kerr-Newman spacetime w.r.t. r for different values of charge e is shown in figure 14.

For a particle outside an ergosphere, to execute circular motion, both V_{eff} and its first derivative with respect to r must vanish. Which gives

$$\left[\begin{aligned} & \left\{ (r(r - 2M) - e^2) r^5 + a^2 (2e^4 - 2r(2M + r)e^2 + r^4) r \right\} \left\{ - \left\{ (2r - 2M) ((r(r - 2M) - e^2) r^5 + a^2 (2e^4 - 2r(2M + r)e^2 + r^4) r) - ((e^2 + r(r - 2M)) \mathcal{E}^2 r^{10}) + (e^2 + (2M - r)r)^2 (\mathcal{L}^2 + r^2) r^6 + 2a^3 \mathcal{L} (2Mr - e^2) \mathcal{E} r^6 + 2a \mathcal{L} (2Mr - e^2) (e^2 + r(r - 2M)) \mathcal{E} r^6 + a^2 ((e^4 - 4Mr e^2 - 2r^4 + 4M^2 r^2) \mathcal{E}^2 r^4 + 2(r(r - 2M) - e^2) (2e^4 - 2r(2M + r)e^2 + r^4) r^2 + \mathcal{L}^2 (-4e^6 + 4r(2M + r)e^4 - 3r^4 e^2 + r^5 (r - 2M))) r^2 + a^4 ((e^2 - r(2M + r)) \mathcal{E}^2 r^6 + (2e^4 - 2r(2M + r)e^2 + r^4)^2) \right\} - 2(a^2 + e^2 + r(r - 2M)) ((r(7r - 12M) - 5e^2) r^4 + a^2 (2e^4 - 2r(4M + 3r)e^2 + 5r^4)) - ((e^2 + r(r - 2M)) \mathcal{E}^2 r^{10}) + (e^2 + (2M - r)r)^2 (\mathcal{L}^2 + r^2) r^6 + 2a^3 \mathcal{L} (2Mr - e^2) \mathcal{E} r^6 + 2a \mathcal{L} (2Mr - e^2) (e^2 + r(r - 2M)) \mathcal{E} r^6 + a^2 ((e^4 - 4Mr e^2 - 2r^4 + 4M^2 r^2) \mathcal{E}^2 r^4 + 2(r(r - 2M) - e^2) (2e^4 - 2r(2M + r)e^2 + r^4) r^2 + \mathcal{L}^2 (-4e^6 + 4r(2M + r)e^4 - 3r^4 e^2 + r^5 (r - 2M))) r^2 + a^4 ((e^2 - r(2M + r)) \mathcal{E}^2 r^6 + (2e^4 - 2r(2M + r)e^2 + r^4)^2) + 2(a^2 + e^2 + r(r - 2M)) ((r(r - 2M) - e^2) r^5 + a^2 (2e^4 - 2r(2M + r)e^2 + r^4) r) \left\{ (5e^2 + r(6r - 11M)) \mathcal{E}^2 r^9 + 2a^3 \mathcal{L} (3e^2 - 7Mr) \mathcal{E} r^5 + 2a \mathcal{L} (3e^4 + 2r(2r - 7M)e^2 + Mr^2 (16M - 9r)) \mathcal{E} r^5 + a^2 (8r^2 e^6 - 3r^4 (\mathcal{E}^2 + 8)e^4 + 2r^4 (-24M^2 + 7r \mathcal{E}^2 M + 12r^2) e^2 + \mathcal{L}^2 (4e^6 - 4r(3M + 2r)e^4 + 9r^4 e^2 + r^5 (7M - 4r)) + 2e^6 (5(\mathcal{E}^2 - 1)r^2 + 9Mr - 8M^2 E^2)) r - r^5 (e^2 + (2M - r)r) ((3e^2 + r(8M - 5r)) \mathcal{L}^2 + 2r^2 (2e^2 + r(5M - 3r))) + a^4 (r^5 (r(7M + 4r) - 3e^2) \mathcal{E}^2 - 4(-2e^4 + 2r(2M + r)e^2 - r^4) (Me^2 + (e - r)r(e + r))) \right\} \right\} \end{aligned} \right] = 0,$$

as a necessary condition. We can justify this equation by four exclusive proofs in this paper, check, for example: equations (7), (53), (69) and (70). The roots of this equation are beyond the scope of this paper.

As for other black holes, the evaluation of ISCO for neutral and charged particles in the Kerr-Newman spacetime is difficult to carry out with the present method. The problem has been studied by the Hamilton Jacobi method by others; see [5, 13]. We have, however, tried to study the variation of effective potential of Kerr-Newman black hole w.r.t. r_{ISCO} for different values of energy \mathcal{E} , see figure 15. We also investigated the variation of r_{ISCO} with V for different values of Kerr parameter a and the variation of r_{ISCO} with the black hole charge for Kerr parameter $a = 0.1$ in different potential depths, see figure 17.

VI. CONCLUSION

We have studied the motion of particles, both neutral and charged, around different black holes. We started with the Schwarzschild black hole, then the Kerr black hole followed by the Reissner-Nordström black hole and the Kerr-Newman black hole. For the Schwarzschild black hole, we concluded that the closest distance that a particle can revolve around the black hole without falling into it is $6M$ and it loses 5.7% of its rest mass energy before finally spiraling into the ISCO — as the existence of ISCO around a densely compact object is a purely relativistic phenomenon, therefore, any intuitional conclusion one might have about its behavior turns out to be invalid. This also suggests that, indeed, by gravitational radiative processes, in the astrophysically plausible phenomenon, large amounts of energy, as much as 42%, can be radiated. The ISCO of Schwarzschild black hole in electric and magnetic fields were analyzed; we concluded that whenever the magnitude of charge ($|q|$) > 0 the radius of ISCO increases; we further deduced the following

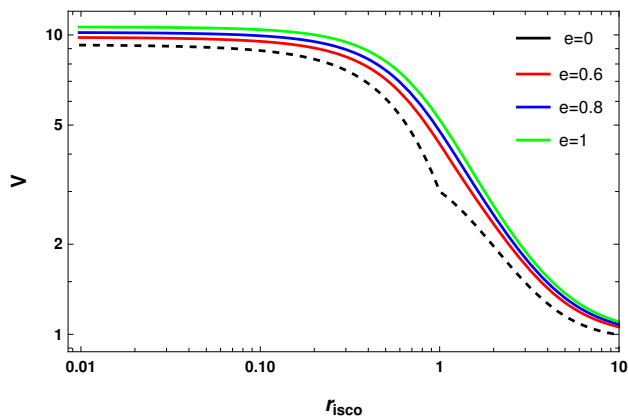


FIG. 16. The variation of r_{ISCO} with V for different values of Kerr parameter a .

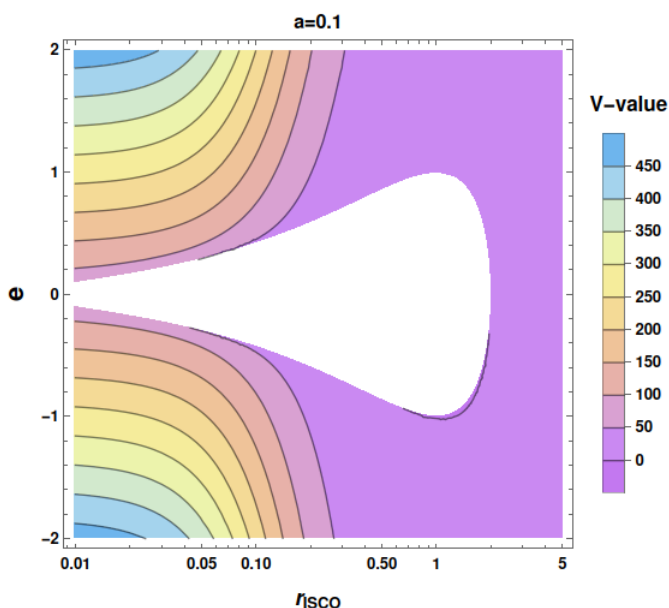


FIG. 17. The variation of r_{ISCO} with the charge of blackhole for Kerr parameter $a = 0.1$ in different potential depths.

effects of the magnetic field on radius (r_{ISCO}): it brings the radius of ISCO closer to the coordinate singularity, it makes the maximum value of charge always greater than M for which r_{ISCO} exists.

After extending the same method to Kerr black holes, a few interesting results emerged: the r_{ISCO} , for neutral particles, lies in the interval $[M, 9M]$. A particle entering the ISCO region of a Kerr spacetime will release an energy fraction, up-to 19%, of its rest mass energy, before finally spiraling into this special orbit. For charged particles orbiting the Kerr spacetime, we saw that an increase in the coupling of black hole and test particle charge

sharpens the ISCO region and stabilizes the angular momentum. We checked by putting $a = 0$ in the dynamical equations of the Kerr black hole that they, as expected, reduces the Kerr spacetime solution to the Schwarzschild one. Evidently, if $(a^2\mathcal{E}^2 - a^2 - \mathcal{L}^2)^2 < 12M^2(\mathcal{L} - a\mathcal{E})^2$ then there is no maxima or minima of $V(r, \mathcal{E}, \mathcal{L})$ which means the particle is trapped and the information is lost. For future research it might be interesting to deduce the same result by using the Heisenberg's uncertainty principle for particles in strong gravitational fields. A very fascinating result emerged from our calculations that is, when $q = M$ a charged particle can be entangled to a Kerr black hole even if they are infinitely apart.

However in our calculations, we have used the weak field approximation, but the charges have the potential to produce curvature comparable to the curvature produced by the black holes' mass near the event horizon, where the weak field approximations likely breakdown.

Similar calculations for Reissner-Nordström black holes, with the condition: $M^2 \geq e^2$, yielded that the highest value of r_{ISCO} for which ISCO solutions can be found when $e = 1$ is $3M$. The size and existence of ISCO for charged particles depend explicitly on how much the spacetime curvature is being tweaked by the black hole charge Q and the coupling product. So, it is conspicuously clear that the charged black holes enhance the stability of circular orbits.

In case of the Kerr-Newman black holes, we again followed the same method, we verified our results by different tests, such as: if we set $e = 0$ and $a \neq 0$, solutions reduced to that of Kerr black hole and if we set $a = 0$ and $e = 0$, that is a charge-less and non-rotating spacetime, it converts the Kerr-Newman into Schwarzschild black hole. We obtained an expression for effective potential for Kerr-Newman black hole, the expression did not contain magnetic parameter b . In future, we would like to create an electromagnetic four potential containing b as well.

We have altogether overlooked an interesting phenomenon called Outermost Stable Circular Orbits (OSCOs) of black holes due to the computational difficulties. For the future research it may be interesting to study the OSCOs of Kerr-Newman black holes. The study of gravitational wave-shift and Doppler shift at the ISCO and OSCO locations around Black holes can be the promising starting point for future research.

ACKNOWLEDGMENTS

The authors duly acknowledge the support and facilities provided by the Central University of Kashmir, J&K —191131, India.

[1] C. W. Misner, K. S. Thorne, and J. A. Wheeler, *Gravitation* (W. H. Freeman, San Francisco, 1973).

[2] B. F. Schutz, *A First Course in General Relativity*, 2nd

- ed. (Cambridge University Press, Cambridge, 2009).
- [3] R. M. Wald, *General Relativity* (University of Chicago Press, Chicago, 1984).
- [4] N. I. Shakura and R. A. Sunyaev, Black holes in binary systems. Observational appearance, *Astronomy and Astrophysics* **24**, 337 (1973).
- [5] K. Schroven and S. Grunau, Innermost stable circular orbit of charged particles in reissner-nordström, kerr-newman, and kerr-sen spacetimes, *Phys. Rev. D* **103**, 024016 (2021).
- [6] G. E. Romero and G. S. Vila, *Introduction to Black Hole Astrophysics*, Lecture Notes in Physics, Vol. 876 (Springer, Berlin, 2014).
- [7] A. M. A. Zahrani, Circular orbits of charged particles around a weakly charged and magnetized schwarzschild black hole, *Phys. Rev. D* **103**, 084008 (2021).
- [8] B. Carter, Black hole equilibrium states, in *Black Holes* (Gordon and Breach, New York, 1973) pp. 57–214.
- [9] M. Zajacek and A. Tursunov, Electric charge of black holes: Is it really always negligible?, arXiv preprint (2019), [arXiv:1904.04654](https://arxiv.org/abs/1904.04654) [astro-ph.HE].
- [10] M. Zajacek, A. Tursunov, A. Eckart, S. Britzen, E. Hackmann, V. Karas, Z. Stuchlik, B. Czerny, and J. A. Zensus, Constraining the charge of Sgr A*, *Journal of Physics: Conference Series* **1258**, 012031 (2019).
- [11] M. Zajacek, A. Tursunov, A. Eckart, and S. Britzen, On the charge of the Galactic centre black hole, *Monthly Notices of the Royal Astronomical Society* **480**, 4408 (2018).
- [12] R. M. Wald, Black hole in a uniform magnetic field, *Phys. Rev. D* **10**, 1680 (1974).
- [13] K. Schroven, E. Hackmann, and C. Lämmerzahl, Test particle motion in the spacetime of a Kerr black hole pierced by a cosmic string, *Phys. Rev. D* **96**, 063015 (2017).
- [14] E. Hackmann and H. Xu, Charged particle motion in a magnetic field in the schwarzschild spacetime: The exact solution, *Physical Review D* **87**, 124030 (2013).
- [15] K. Schwarzschild, Über das gravitationsfeld eines massenpunktes nach der einsteinschen theorie, *Sitzungsberichte der Königlich Preußischen Akademie der Wissenschaften*, 189 (1916), read on 13 January 1916.
- [16] J. J. O’Connor and E. F. Robertson, *Karl schwarzschild - biography*, MacTutor History of Mathematics Archive, University of St Andrews (2003), accessed: 2026-02-28.
- [17] K. Schwarzschild, *On the gravitational field of a point mass according to einstein’s theory*, arXiv preprint physics (1999), translated by S. Antoci and A. Loinger.
- [18] R. Penrose, Gravitational collapse and space-time singularities, *Physical Review Letters* **14**, 57 (1965), published 18 January 1965.
- [19] R. P. Kerr, Gravitational field of a spinning mass as an example of algebraically special metrics, *Physical Review Letters* **11**, 237 (1963).
- [20] H. Reissner, Über die eigengravitation des elektrischen feldes nach der einsteinschen theorie, *Ann. Phys. (Berlin)* **355**, 10.1002/andp.19163550905 (1916).
- [21] G. Nordström, On the energy of the gravitation field in einstein’s theory, *Proc. K. Ned. Akad. Wet.* **20**, 1238 (1918), bibcode: 1918KNAB...20.1238N.
- [22] E. T. Newman *et al.*, Metric of a rotating, charged mass, *J. Math. Phys.* **6**, 918–919 (1965) **6**, 918 (1965).